References

1. Hensch, T. K. (2005) *Nat. Rev. Neurosci.* **6**, 877–888.
2. Tropea, D., Van, Wart, A., and Sur, M. (2009) *Philos. Trans. R. Soc. B* **364**, 341–355.
3. Jiang, B., Huang, Z. J., Morales, B., and Kirkwood, A. (2005) *Brain Res. Brain Res. Rev.* **50**, 126–133.
4. Johnson, J. S., and Newport, E. L. (1989) *Cogn. Psychol.* **21**, 60–99.
5. Feldman, D. E. (2000) *Nat. Neurosci.* **3**, 303–304.
6. Fagiolini, M., Fritschy, J. M., Löw, K., Möhler, H., Rudolph, U., and Hensch, T. K. (2004) *Science* **303**, 1681–1683.
7. Huang, Z. J., Kirkwood, A., Pizzorusso, T., Porciatti, V., Morales, B., Bear, M. F., Maffei, L., and Tonegawa, S. (1999) *Cell* **98**, 739–755.
8. Yazaki-Sugiyama, Y., Kang, S., Câteau, H., Fukai, T., and Hensch, T. K. (2009) *Nature* **462**, 218–221.
9. Sugiyama, S., Di Nardo, A. A., Aizawa, S., Matsuo, I., Volovitch, M., Prochiantz, A., and Hensch, T. K. (2008) *Cell* **134**, 508–520.
10. Harauzov, A., Spolidoro, M., DiCristo, G., De Pasquale, R., Cancedda, L., Pizzorusso, T., Viegi, A., Berardi, N., and Maffei, L. (2010) *J. Neurosci.* **30**, 361–371.
11. Pizzorusso, T., Medini, P., Berardi, N., Chierzi, S., Fawcett, J. W., and Maffei, L. (2002) *Science* **298**, 1248–1251.
12. Fox, K., and Caterson, B. (2002) *Science* **298**, 1187–1189.
13. Bandtlow, C. E., and Zimmermann, D. R. (2000) *Physiol. Rev.* **80**, 1267–1290.
14. Sugahara, K., and Mikami, T. (2007) *Curr. Opin. Struct. Biol.* **17**, 536–545.
15. Kusche–Gullberg, M., and Kjellén, L. (2003) *Curr. Opin. Struct. Biol.* **13**, 605–611.
16. Gama, C. I., Tully, S. E., Sotogaku, N., Clark, P. M., Rawat, M., Vaidehi, N., Goddard, W. A. 3rd., Nishi, A., and Hsieh-Wilson, L. C. (2006) *Nat. Chem. Biol.* **2**, 467–473.
17. Mikami, T., Yasunaga, D., and Kitagawa, H. (2009) *J. Biol. Chem.* **284**, 4494–4499.
18. Nadanaka, S., Kinouchi, H., Taniguchi-Morita, K., Tamura, J., and Kitagawa, H. (2011) *J. Biol. Chem.* **286**, 4199–41208.
19. Sugahara, K., Mikami, T., Uyama, T., Mizuguchi, S., Nomura, K., and Kitagawa, H. (2003) *Curr. Opin. Struct. Biol.* **13**, 612–620.
20. Kitagawa, H., Uyama, T., and Sugahara, K. (2001) *J. Biol. Chem.* **276**, 38721–38726.
21. Izumikawa, T., Uyama, T., Okuura, Y., Sugahara, K., and Kitagawa, H. (2007) *Biochem. J.* **403**, 545–552.
22. Izumikawa, T., Koike, T., Shiozawa, S., Sugahara, K., Tamura, J., and Kitagawa, H. (2008) *J. Biol. Chem.* **283**, 11396–11406.
23. Kitagawa, H., Izumikawa, T., Uyama, T., and Sugahara, K. (2003) *J. Biol. Chem.* **278**, 23666–23671.
24. Uyama, T., Kitagawa, H., Tamura, J., and Sugahara, K. (2002) *J. Biol. Chem.* **277**, 8841–8846.
25. Gotoh, M., Sato, T., Akashima, T., Iwasaki, H., Kameyama, A., Mochizuki, H., Yada, T., Inaba, N., Zhang, Y., Kikuchi, N., Kwon, Y. D., Togayachi, A., Kudo, T., Nishihara, S., Watanabe, H., Kimata, K., and Narimatsu, H. (2002) *J. Biol. Chem.* **277**, 38189–38196.
26. Sato, T., Gotoh, M., Kiyohara, K., Akashima, T., Iwasaki, H., Kameyama, A., Mochizuki, H., Yada, T., Inaba, N. Togayachi, A., Kudo, T., Asada, M., Watanabe, H., Imamura, T., Kimata, K., and Narimatsu, H. (2003) *J. Biol. Chem.* **278**, 3063–3071.
27. Uyama, T., Kitagawa, H., Tanaka, J., Tamura, J., Ogawa, T., and Sugahara, K. (2003) *J. Biol. Chem.* **278**, 3072–3078.
28. Hiraoka, N., Nakagawa, H., Ong, E., Akama, T. O., Fukuda, M. N., and Fukuda, M. (2000) *J. Biol. Chem.* **275**, 20188–20196.
29. Kang, H.-G., Evers, M. R., Xia, G., Baenziger, J. U., and Schachner, M. (2002) *J. Biol. Chem.* **277**, 34766–34772.
30. Yamauchi, S., Mita, S., Matsubara, T., Fukuta, M., Habuchi, H., Kimata, K., and Habuchi, O. (2000) *J. Biol. Chem.* **275**, 8975–8981.
31. Mikami, T., Mizumoto, S., Kago, N., Kitagawa, H., and Sugahara, K. (2003) *J. Biol. Chem.* **278**, 36115–36127.
32. Fukuta, M., Uchimura, K., Nakashima, K., Kato, M., Kimata, K., Shinomura, T., and Habuchi, O. (1995) *J. Biol. Chem.* **270**, 18575–18580.
33. Tsutsumi, K., Shimakawa, H., Kitagawa, H., and Sugahara, K. (1998) *FEBS Lett.* **441**, 235–241.
34. Ohtake, S., Ito, Y., Fukuta, M., and Habuchi, O. (2001) *J. Biol. Chem.* **276**, 43894–43900.
35. Kobayashi, M., Sugumaran, G., Liu, J., Shworak, N. W., Silbert, J. E., and Rosenberg, R. D. (1999) *J. Biol. Chem.* **274**, 10474–10480.
36. Galtrey, C.M., and Fawcett, J. W. (2007) *Brain Res. Rev.* **54**, 1–18.
37. Davies, S. J., Fitch, M. T., Memberg, S. P., Hall, A. K., Raisman, G., and Silver, J. (1997) *Nature* **390**, 680–683.
38. Bradbury, E. J., Moon, L. D., Popat, R. J., King, V. R., Bennett, G. S., Patel, P. N., Fawcett, J. W., and McMahon, S. B. (2002) *Nature* **416**, 636–640.
39. Shen, Y., Tenney, A. P., Busch, S. A., Horn, K. P., Cuascut, F. X., Liu, K., He, Z., Silver, J., and Flanagan, J. G. (2009) *Science* **326**, 592–596.
40. Coles, C. H., Shen, Y., Tenney, A. P., Siebold, C., Sutton, G. C., Lu, W., Gallagher, J. T., Jones, E. Y., Flanagan, J. G., and Aricescu, A. R. (2011) *Science* **332**, 484–488.
41. Properzi, F., Carulli, D., Asher, R. A., Muir, E., Camargo, L. M., van Kuppevelt, T. H., ten Dam, G. B., Furukawa, Y., Mikami, T., Sugahara, K., Toida, T., Geller, H. M., and Fawcett, J. W. (2005) *Eur. J. Neurosci.* **21**, 378–390.
42. Wiesel, T. N., and Hubel, D. H. (1963) *J. Neurophysiol.* **26**, 1003–1017.
43. Gordon, J. A., and Stryker, M. P. (1996) *J. Neurosci.* **16**, 3274–3286.
44. Frenkel, M. Y., and Bear, M. F. (2004) *Neuron* **44**, 917–923.
45. Sawtell, N. B., Frenkel, M. Y., Philpot, B. D., Nakazawa, K., Tonegawa, S., and Bear, M. F. (2003) *Neuron* **38**, 977–985.
46. Sato, M., and Stryker, M. P. (2008) *J. Neurosci.* **28**, 10278–10286.
47. Bavelier, D., Levi, D. M., Li, R. W., Dan, Y., and Hensch, T. K. (2010) *J. Neurosci.* **30**, 14964–14971.
48. Morishita, H., Miwa, J. M., Heintz, N., and Hensch, T. K. (2010) *Science* **330**, 1238–1240.
49. McGee, A. W., Yang, Y., Fischer, Q. S., Daw, N. W., and Strittmatter, S. M. (2005) *Science* **309**, 2222–2226.
50. Kitagawa, H., Tsutsumi, K., Tone, Y., and Sugahara, K. (1997) *J. Biol. Chem.* **272**, 31377–31381.
51. Celio, M. R., Spreafico, R., De Biasi, S., and Vitellaro-Zuccarello, L. (1998) *Trends Neurosci.* **21**, 510–515.
52. Dours–Zimmermann M. T., Maurer, K., Rauch, U., Stoffel, W., Fässler, R., and Zimmermann, D. R. (2009) *J. Neurosci.* **29**, 7731–7742.
53. Zhou, X. H., Brakebusch, C., Matthies, H., Oohashi, T., Hirsch, E., Moser, M., Krug, M., Seidenbecher, C. I., Boeckers, T. M., Rauch, U., Buettner, R., Gundelfinger, E. D., and Fässler, R. (2001) *Mol. Cell. Biol.* **21**, 5970–5978.
54. Brakebusch, C., Seidenbecher, C. I., Asztely, F., Rauch, U., Matthies, H., Meyer, H., Krug, M., Böckers, T. M., Zhou, X., Kreutz, M. R., Montag, D., Gundelfinger, E. D., and Fässler, R. (2002) *Mol. Cell. Biol.* **22**, 7417–7327.

55. Giamanco, K. A., Morawski, M., and Matthews, R. T. (2010) *Neuroscience* **170**, 1314–1327.
56. Matthews, R. T., Kelly, G. M., Zerillo, C. A., Gray, G., Tiemeyer, M., and Hockfield, S. (2002) *J. Neurosci.* **22**, 7536–7547.
57. Lander, C., Zhang, H., and Hockfield, S. (1998) *J. Neurosci.* **18**, 174–183.
58. Watanabe, H., Kimata, K., Line, S., Strong, D., Gao, L. Y., Kozak, C. A., and Yamada, Y. (1994) *Nat. Genet.* **7**, 154–157.
59. Carulli, D., Rhodes, K. E., and Fawcett, J. W. (2007) *J. Comp. Neurol.* **501**, 83–94.
60. Carulli, D., Pizzorusso, T., Kwok, J. C., Putignano, E., Poli, A., Forostyak, S., Andrews, M. R., Deepa, S. S., Glant, T. T., and Fawcett, J. W. (2010) *Brain* **133**, 2331–2347.
61. Weber, P., Bartsch, U., Rasband, M. N., Czaniera, R., Lang, Y., Bluethmann, H., Margolis, R. U., Levinson, S. R., Shrager, P., Montag, D., and Schachner, M. (1999) *J. Neurosci.* **19**, 4245–4262.
62. Saghatelyan, A. K., Dityatev, A., Schmidt, S., Schuster, T., Bartsch, U., and Schachner, M. (2001) *Mol. Cell. Neurosci.* **17**, 226–240.
63. Erisir, A., and Dreusicke, M. (2005) *J. Comp. Neurol.* **485**, 11–31.
64. Chang, M. C., Park, J. M., Pelkey, K. A., Grabenstatter, H. L., Xu, D., Linden, D. J., Sutula, T. P., McBain, C. J., and Worley, P. F. (2010) *Nat. Neurosci.* **13**, 1090–1097.
65. Frischknecht, R., Heine, M., Perrais, D., Seidenbecher, C. I., Choquet, D., and Gundelfinger, E. D. (2009) *Nat. Neurosci.* **12**, 897–904.
66. Kochlamazashvili, G., Henneberger, C., Bukalo, O., Dvoretskova, E., Senkov, O., Lievens, P. M., Westenbroek, R., Engel, A. K., Catterall, W. A., Rusakov, D. A., Schachner, M., and Dityatev, A. (2010) *Neuron* **67**, 116–128.
67. Gogolla, N., Caroni, P., Lüthi, A., and Herry, C. (2009) *Science* **325**, 1258–1261.
68. Lewis, D. A., Hashimoto, T., and Volk, D.W. (2005) *Nat. Rev. Neurosci.* **6**, 312–324.
69. Fazzari, P., Paternain, A. V., Valiente, M., Pla, R., Luján, R., Lloyd, K., Lerma, J., Marín, O., and Rico, B. (2010) *Nature* **464**, 1376–1380.
70. Pantazopoulos, H., Woo, T. U., Lim, M. P., Lange, N., and Berretta, S. (2010) *Arch. Gen. Psychiatry* **67**, 155–166.

Profile of the Authors

Shinji Miyata received his Ph.D. degree from the Graduate School of Bioagricultural Sciences, the Nagoya University in 2006 under the supervision of Prof. Ken Kitajima. He did postdoctoral research at the Scripps Institution of Oceanography, the University of California San Diego with Prof. Victor D. Vacquier (2006–2007). From 2007, he joined Prof. Hiroshi Kitagawa's laboratory in the Kobe Pharmaceutical University, as a postdoctoral fellow. His research interest is focused on biological function of chondroitin sulfate chains in the central nervous system.

Hiroshi Kitagawa graduated from the Faculty of Pharmaceutical Sciences, Kyoto University in 1986. He received his Ph.D. in Biochemistry in 1991 from Kyoto University. He did his doctoral work in the laboratories of Prof. Ikuo Yamashina and Prof. Toshisuke Kawasaki on the purification and characterization of cancer-associated carbohydrate antigens by using monoclonal antibodies raised against human cancer cells. He went on to do post-doctoral work with Dr. James C. Paulson at Cytel Corporation and Scripps Research Institute. In Dr. Paulson's laboratory, he worked on the molecular cloning and characterization of several sialyltransferases. In 1994 he obtained an assistant professor position at the Department of Biochemistry, Kobe Pharmaceutical University, where he started to work on the structure and biosynthesis of sulfated glycosaminoglycans. He was promoted to associate professor in 2000 and full professor in 2005. He received the young scientist award of the Japanese Society of Carbohydrate Research in 1999, the PSJ (Pharmaceutical Society of Japan) award for young scientists in 2001, and the young investigator award of the Japanese Biochemical Society in 2002. He has continued to work on the functions and the control of the biosynthesis and degradation of sulfated glycosaminoglycans, aiming to clarify the causes of various disorders.

Chondroitin 4-O-sulfotransferase-2 regulates the number of chondroitin sulfate chains initiated by chondroitin N-acetylgalactosaminyltransferase-1

Tomomi IZUMIKAWA, Toshiyasu KOIKE and Hiroshi KITAGAWA[1]

Department of Biochemistry, Kobe Pharmaceutical University, Higashinada-ku, Kobe 658-8558, Japan

Recently, it has been shown that a deficiency in ChGn-1 (chondroitin N-acetylgalactosaminyltransferase-1) reduced the numbers of CS (chondroitin sulfate) chains, leading to skeletal dysplasias in mice. Although these results indicate that ChGn-1 regulates the number of CS chains, the mechanism mediating this regulation is not clear. ChGn-1 is thought to initiate CS biosynthesis by transferring the first GalNAc (N-acetylgalactosamine) to the tetrasaccharide in the protein linkage region of CS. However, in vitro chondroitin polymerization does not occur on the non-reducing terminal GalNAc-linkage pentasaccharide structure. In the present study we show that several different heteromeric enzyme complexes composed of different combinations of four chondroitin synthase family members syn- thesized more CS chains when a GalNAc-linkage pentasaccharide structure with a non-reducing terminal 4-O-sulfation was the CS acceptor. In addition, C4ST-2 (chondroitin 4-O-sulfotransferase- 2) efficiently transferred sulfate from 3′-phosphoadenosine 5′- phosphosulfate to position 4 of non-reducing terminal GalNAc- linkage residues, and the number of CS chains was regulated by the expression levels of C4ST-2 and of ChGn-1. Taken together, the results of the present study indicate that C4ST-2 plays a key role in regulating levels of CS synthesized via ChGn-1.

Key words: chondroitin sulfate, glycosaminoglycan, glycosyl- transferase, proteoglycan, sulfotransferase.

INTRODUCTION

CSs (chondroitin sulfates) are covalently bound to specific serine residues in the core regions of many proteins through a common carbohydrate–protein linkage tetrasaccharide GlcAβ1-3Galβ1-3Galβ1-4Xylβ1-O-Ser. Following the complete synthesis of the linkage-region tetrasaccharide, the first GalNAc (N-acetylgalactosamine) residue is transferred to a GlcA (glucuronic acid) residue in the linkage-region tetrasaccharide, triggering the synthesis of CS. Next, GlcA and GalNAc residues are alternately transferred on to growing CS chains, resulting in the formation of the polymer sugar backbone of CS [1]. After the synthesis of the CS sugar backbone on this tetrasaccharide, numerous modifications, including sulfation, occur under tight spatio-temporal regulation producing mature and functional GAG (glycosaminoglycan) chains that exert specific biological functions that are dependent on their specific structures.

To date, six glycosyltransferases involved in the biosynthesis of CS have been cloned. We and others have identified the six chondroitin-synthesizing enzymes: ChSy (chondroitin synthase)- 1, ChSy-2, ChSy-3, ChPF (chondroitin-polymerizing factor) and ChGn (chondroitin GalNAc transferase)-1 and -2 [2–9]. ChSy-1, ChSy-2 and ChSy-3 show dual glycosyltransferase activities, GlcAT-II (GlcA transferase II) and GalNAcT-II (GalNAc transferase II), that are responsible for synthesizing the repeating disaccharide units of CS [2–4], and ChGn-1 and -2 catalyse chain initiation and elongation, exhibiting activities of GalNAcT-I and -II [6–9]. In addition, seven sulfotransferases involved in the sulfation of CS, including four sulfotrans- ferases involved in the sulfation of position 4 of the GalNAc residue, have been cloned [10]. C4STs (chondroitin 4-O- sulfotransferases)-1, -2 and -3 are responsible for the sulfation of position 4 of the GalNAc residues in CS, whereas D4ST-1 (dermatan 4-O-sulfotransferase-1) catalyses the transfer of sulfate residues to GalNAc residues located next to IdoUA (iduronic acid) residues in DS (dermatan sulfate) [11–15]. C6ST-1 (chondroitin 6-O-sulfotransferase-1) transfers sulfate to position 6 of GalNAc residues [16,17]. The 2-O-sulfation of GlcA and IdoUA is cata- lysed by uronyl 2-O-sulfotransferase [18]. GalNAc4S-6ST (Gal- NAc 4-sulfate 6-O-sulfotransferase) transfers a sulfate residue to position 6 of GalNAc(4-O-sulfate) formed by C4ST [19].

Previously, we demonstrated that chondroitin is polymerized with alternating GalNAc and GlcA residues on the linkage- region tetrasaccharide of α-TM (α-thrombomodulin) when any two of four proteins, ChSy-1, ChSy-2, ChSy-3 and ChPF, were co-expressed [3–5]. These results indicated that ChGn-1 and ChGn-2, both of which have both GalNAcT-I and -II activity, were dispensable for chondroitin polymerization on the linkage- region tetrasaccharide [3–5]; however, recently it was shown that a deficiency in ChGn-1 reduced the number of CS chains, leading to skeletal dysplasias in mice [20]. Taken together, these results indicate that the transfer of a single GalNAc residue to the tetrasaccharide linkage region by ChGn-1 and the activity of chondroitin polymerases comprising any two of the ChSy- 1, ChSy-2, ChSy-3 and ChPF proteins are both important for efficient biosynthesis of CS chains.

Given these findings, we hypothesized that the non-reducing terminal GalNAc-linkage structure formed by ChGn-1 would markedly enhance the number of CS chains produced by chondroitin polymerases comprising any two of the ChSy-1, ChSy-2, ChSy-3 and ChPF proteins (Figure 1). However, the results of the present study demonstrated that a non-reducing terminal GalNAc-linkage structure did not serve as a chondroitin polymerization substrate. In the present paper we report that
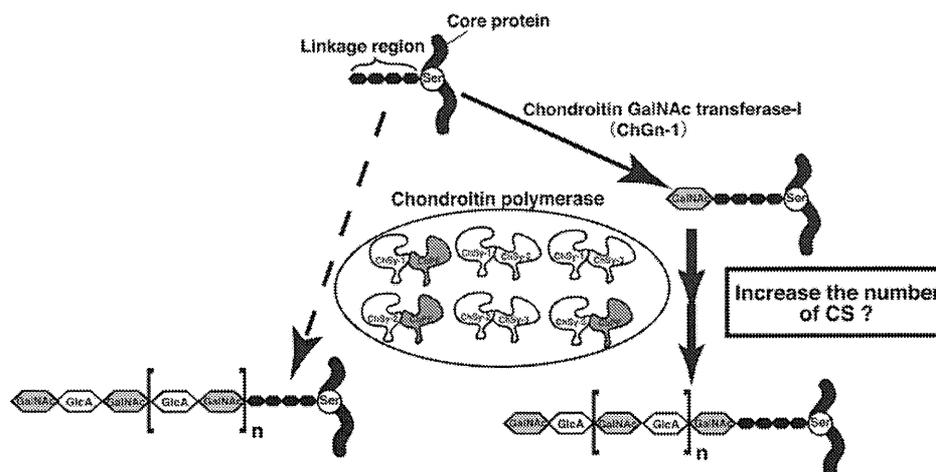

Figure 1   Initiation of CS polymerization

CS is synthesized as proteoglycans on specific serine residues in the GAG-protein linkage region, GlcAβ1-3Galβ1-3Galβ1-4Xylβ1-O-Ser. Following the complete synthesis of the linkage-tetrasaccharide sequence, the transfer of a single GalNAc residue to the tetrasaccharide linkage region by any two of ChSy-1, ChSy-2, ChSy-3 or ChPF (broken line), or by ChGn-1 (solid line) initiates the assembly of CS. Thus it was expected that the non-reducing terminal GalNAc-linkage structure formed by ChGn-1 would markedly enhance the number of CS chains produced by chondroitin polymerases, meaning any two of ChSy-1, ChSy-2, ChSy-3 and ChPF.

a non-reducing terminal GalNAc(4-O-sulfate)-linkage structure on CS resulted in an increase in the number of CS chains that were synthesized by multiple enzyme complexes comprising combinations of four ChSy family members and that C4ST-2 was involved in the mechanism that resulted in an increase in the number of CS chains that was mediated by ChGn-1.

EXPERIMENTAL

Materials

UDP-[^{3}H]GalNAc (10 Ci/mmol) was purchased from NEN Life Science Products, and ^{35}S-labelled PAPS (3'-phosphoadenosine 5'-phosphosulfate) (1.69 mCi/mmol) was purchased from PerkinElmer Life Sciences. Unlabelled UDP-GlcA, UDP-GalNAc and PAPS were obtained from Sigma. Chondroitinase ABC isolated from *Proteus vulgaris* (EC 4.2.2.20) and chondroitinase ACII isolated from *Arthrobacter aurescens* (EC 4.2.2.5) were purchased from Seikagaku. Superdex™ Peptide HR10/30 and Superdex™ 200 10/300 GL columns were purchased from Amersham Pharmacia Biotech. α-TM with a truncated linkage-region tetrasaccharide, GlcAβ1-3Galβ1-3Galβ1-4Xyl, was purified and structurally characterized as described previously [21,22].

Polymerization assay and identification of polymerization reaction products

First, a GalNAc transfer reaction was conducted; α-TM that contained the linkage-region tetrasaccharide GlcAβ1-3Galβ1-3Galβ1-4Xyl (1 nmol) was used as an acceptor in the incubation mixture, which contained the following constituents in a total volume of 20 μl: 10 μl of the soluble form of ChGn-1-bound beads [6] as the enzyme source, 0.25 mM UDP-GalNAc or UDP-[^{3}H]GalNAc (2×10^5 d.p.m.), 100 mM Mes buffer (pH 5.8) and 10 mM MnCl$_2$. Then, the reaction products were separated by gel-filtration chromatography on a Superdex™ peptide column that had been equilibrated and eluted with 0.25 M NH$_4$HCO$_3$/7 % propan-1-ol. Next, 4-O-sulfation of the GalNAc residue was

performed using GalNAc-TM (GalNAcβ1-4GlcAβ1-3Galβ1-3Galβ1-4Xylβ1-O-TM) (1 nmol) as an acceptor in an incubation mixture, which contained the following constituents in a total volume of 30 μl: 10 μl of the soluble form of C4ST-2-bound beads [15] as the enzyme source, 50 mM imidazole/HCl (pH 6.8), 2 mM dithiothreitol and 10 μM [^{35}S]PAPS (3×10^5 d.p.m.). Then, the reaction products were separated by gel-filtration chromatography on a Superdex™ peptide column that had been equilibrated and eluted with 0.25 M NH$_4$HCO$_3$/7 % propan-1-ol. The fractions containing the enzyme reaction products were pooled and evaporated to dryness. The isolated reaction products were used as substrates for polymerization reactions. Polymerization reactions were simultaneously incubated in parallel in reaction mixtures containing the following constituents in a total volume of 20 μl: 1 nmol of [^{3}H]GalNAc-TM or [^{35}S]GalNAc(4-O-sulfate)β1-4GlcAβ1-3Galβ1-3Galβ1-4Xylβ1-O-TM {[^{35}S]GalNAc(4S)-TM}, 0.25 mM UDP-GalNAc, 0.25 mM UDP-GlcA, 100 mM Mes buffer (pH 6.5), 10 mM MnCl$_2$, and 10 μl of the soluble form of ChSy-1–ChPF-, ChSy-1–ChSy-2-, ChSy-1–ChSy-3-, ChSy-2–ChPF-, ChSy-2–ChSy-3- or ChSy-3–ChPF-bound beads. The mixtures were incubated at 37 °C overnight, and the ^{3}H- or ^{35}S-labelled products were then separated by gel-filtration chromatography on a Superdex™ 200 column equilibrated and eluted with 0.25 M NH$_4$HCO$_3$/7 % propan-1-ol. Fractions (0.4 ml each) were collected at a flow rate of 0.4 ml/min, and radioactivity was measured with a liquid scintillation counter.

Establishment of an expression vector for ChGn-1 and preparation of cells that stably expressed ChGn-1

A cDNA fragment encoding *ChGn-1* (HUGO nomenclature *CSGALNACT1*) was amplified by RT (reverse transcription) using total RNA from G361 human melanoma cells (A.T.C.C. CRL-1424) as a template, and the forward primer 5'-CGGGAT-CCTCTGGACGCATGGCTGATTC-3' and the reverse primer 5'-CGGGATCCCAGCTGGCACTGCCCAGG-3'; each primer contained a BamHI site. PCR was performed with KOD-Plus DNA polymerase (TOYOBO) for 30 cycles at 94 °C for 30 s, 58 °C for 42 s and 68 °C for 180 s in 5 % (v/v) DMSO. The

PCR fragments were subcloned into the BamHI sites of the pCMV expression vector (Invitrogen). The insert of the plasmid constructs (pCMV-ChGn-1) was confirmed by DNA sequencing. The expression plasmid (6.7 μg) was transfected into L and sog9 cells on 100-mm plates using FuGENE® 6 (Roche Applied Science), according to the manufacturer's protocol. Transfectants were cultured in the presence of 300 μg/ml G418, after which the resistant colonies were picked and propagated for experiments.

ChGn-1 silencing in L cells was performed using MISSION shRNA (short hairpin RNA) (Sigma). Plasmids (6.7 μg) encoding shRNA were transfected into L cells on 100-mm plates using FuGENE® 6 according to the manufacturer's protocol. Transfectants were cultured in the presence of 0.4 mg/ml puromycin. Resistant colonies were then picked and propagated for experiments.

Quantitative real-time RT–PCR

Total RNA was extracted from L cells or sog9 cells using TRIzol® reagent (Invitrogen). The cDNA was synthesized from $\sim$1 μg of total RNA using Moloney murine leukemia virus reverse transcriptase (Promega) and oligo(dT)$_{20}$-M4 adaptor primers (TaKaRa). The primer sequences used were as follows: ChGn-1, forward primer 5'-AGAA-GAAATAAATGAAGTCAAAGGAATAC-3' and reverse primer 5'-GAAGTAGTAGTCCACATCACAG-3'; ChGn-2, forward primer 5'-CCTAGAATCTGTCACCAGT-3' and reverse primer 5'-GTTAAGGAATTCGGCTGAGAAATA-3'; C4ST-1, forward primer 5'-ACCTCGTGGGCAAGTATGAG-3' and reverse primer 5'-TCTGGAAGAACTCCGTGGTC-3'; C4ST-2, forward primer 5'-ATCAGCATCACCAGCAACA-3' and reverse primer 5'-TGTGGCCTGGAGAGAGAC-3'; and GAPDH (glyceraldehyde-3-phosphate dehydrogenase), forward primer 5'-CATC-TGAGGGCCCACTG-3' and reverse primer 5'-GAGGC-CATGTAGGCCATGA-3'. Quantitative real-time RT–PCR was performed using a FastStart DNA Master plus SYBR Green I kit (Roche Diagnostics) in a LightCycler ST300 (Roche Diagnostics). The expression levels of *ChGn-1, ChGn-2, C4ST-1* (HUGO nomenclature *CHST11*) or *C4ST-2* (HUGO nomenclature *CHST12*) mRNA were normalized to that of the *GAPDH* transcript.

Derivatization of GAGs from L and sog9 cells using a fluorophore, 2-aminobenzamide

GAGs from L and sog9 cells were prepared as described previously [23]. The purified GAG fraction was digested with chondroitinase ABC, and the digests were then derivatized with 2-aminobenzamide and analysed by HPLC as described previously [24].

Gel-filtration chromatography of GAGs

To measure the GAG chain lengths, the purified GAG fraction was subjected to reductive β-elimination using NaBH$_4$/NaOH, and then analysed by gel-filtration chromatography on a Superdex™ 200 column (10 mm×300 mm) eluted with 0.2 M ammonium bicarbonate at a flow rate of 0.4 ml/min. Fractions were collected at 3-min intervals, freeze-dried and digested with chondroitinase ABC. The digests were derivatized with 2-aminobenzamide, and then analysed by HPLC on an amine-bound PA-03 column, as described previously [24,25].

Expression of the soluble forms of the recombinant C4ST-1, C4ST-2 and D4ST-1, and identification of the reaction products

Each expression plasmid (6.0 μg) was transfected into COS-1 cells on 100-mm plates using FuGENE® 6 according to the manufacturer's protocol and as described previously [15]. At 2 days after transfection, 1 ml of the culture medium was collected and incubated with 10 μl of IgG–Sepharose (Amersham Pharmacia Biotech) for 1 h at 4°C. The beads recovered by centrifugation (150 *g* at 4°C for 5 min) were washed with and then resuspended in the assay buffer [50 mM imidazole/HCl (pH 6.8)], and the washed beads were tested for sulfotransferase activity. The assays used to detect sulfotransferase have been described previously [15] and were used with slight modifications. Briefly, the standard reaction mixture (30 μl) contained 10 μl of resuspended beads, 50 mM imidazole/HCl (pH 6.8), 2 mM dithiothreitol, 10 μM [^{35}S]PAPS (3×10^5 d.p.m.) and 1 nmol of GalNAc-TM as an acceptor substrate. The reaction mixtures were incubated at 37°C overnight and subjected to gel filtration using the Superdex™ peptide column with 0.25 M NH$_4$HCO$_3$/7 % propan-1-ol as the eluent. The radioactive fractions containing the enzyme reaction products were pooled and evaporated to dryness. The isolated reaction products were subjected to reductive β-elimination using NaBH$_4$/NaOH, and then digested with chondroitinase AC-II. The enzymatically digested products were analysed using the Superdex™ peptide column with 0.25 M NH$_4$HCO$_3$/7 % propan-1-ol as the eluent.

Construction of an expression vector for C4ST-2 and preparation of cells that stably expressed C4ST-2

A cDNA fragment encoding *C4ST-2* was amplified using mouse heart Marathon-Ready cDNA (Clontech) as a template by two-round PCR using specific primer sets. The first PCR was performed with the forward primer 5'-CCAGCTGTG-CACAAGGCTGA-3' and the reverse primer 5'-TGCCTG-TCACACCAGGAAGC-3', followed by nested PCR with the nested forward primer 5'-GCACAAGGCTGAAGTGAAGG-3' and the reverse primer 5'-AAGGAAGCCAGGAGAGAACC-3'. Each PCR was carried out using KOD-Plus in the presence of 5 % (v/v) DMSO and was subjected to 30 cycles at 94°C for 30 s, 55°C for 42 s, and 68°C for 2.5 min. Amplified cDNA fragments of the expected size ($\sim$1.4 kb) were purified and subcloned into pGEM®-T Easy vectors (Promega). The cDNA encoding a full-length form of C4ST-2 from pGEM®-T Easy-C4ST-2 vectors was digested with EcoRI and subcloned into the EcoRI site of a pCMV expression vector. The insert of the plasmid constructs (pCMV-C4ST-2) was confirmed by DNA sequencing. The expression plasmid (6.7 μg) was transfected into L or sog9 cells on 100-mm plates using FuGENE® 6, according to the manufacturer's protocol. Transfectants were cultured in the presence of 300 μg/ml G418, after which the resistant colonies were picked and propagated for experiments.

RESULTS

A GalNAc-linkage structure did not serve as a chondroitin polymerization substrate

Recently, it has been shown that *ChGn-1*-deficient mice showed a 50 % decrease in CS levels in developing cartilage and a delay in cartilage development [20]. These results indicated that the non-reducing terminal GalNAc-linkage structure formed by ChGn-1 could markedly enhance the production of CS chains mediated by chondroitin polymerases that synthesize the CS backbone. Previously, we demonstrated that chondroitin
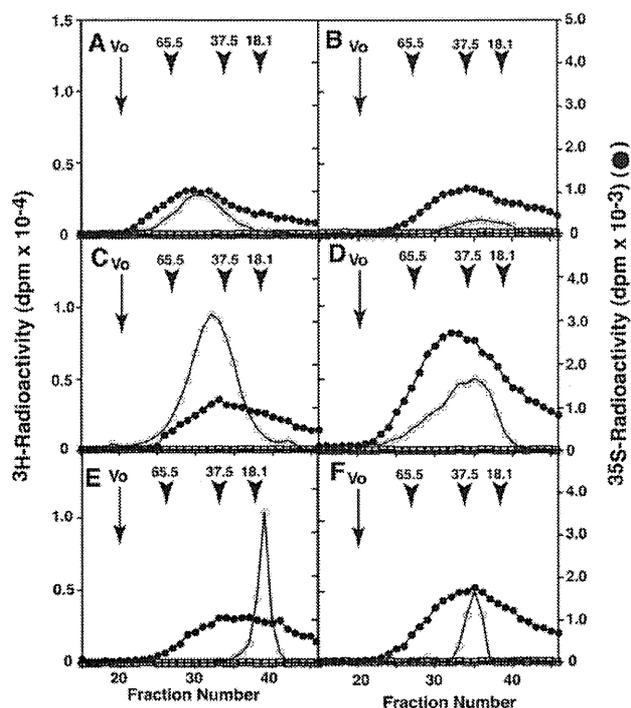
Figure 2   Comparison of CS chain lengths polymerized using various acceptors containing different non-reducing terminal structures

α-TM (O), which is a part-time proteoglycan and bears a truncated linkage region tetrasaccharide (GlcAβ1-3Galβ1-3Galβ1-4Xyl), [^{3}H]GalNAc-TM ($\square$), which bears the non-reducing terminal GalNAc-linkage pentasaccharide, and the ^{35}S-labelled pentasaccharide TM [^{35}S]GalNAc(4S)-TM (●), were each tested as acceptors of polymerization reactions, and the co-expressed ChSy-1 and ChPF (**A**), ChSy-1 and ChSy-2 (**B**), ChSy-1 and ChSy-3 (**C**), ChSy-2 and ChPF (**D**), ChSy-2 and ChSy-3 (**E**), and ChSy-3 and ChPF (**F**) were used as the enzyme source, as described in the Experimental section. ^{3}H-Labelled or ^{35}S-labelled polymerization reaction products were first isolated by gel filtration, subjected to reductive β-elimination using NaBH$_4$/NaOH, and then rechromatographed on a Superdex™ 200 column with 0.25 M NH$_4$HCO$_3$/7 % propan-1-ol as the eluent. Arrowheads numbered 65.5, 37.5 and 18.1 indicate the eluted position of 65.5 kDa saccharides, 37.5 kDa saccharides and 18.1 kDa saccharides respectively, derived from commercial polysaccharides of known sizes (dextran average molecular masses of 200 kDa, 65.5 kDa, 37.5 kDa and 18.1 kDa; all from Sigma). The total volume was a fraction of ~60 (not shown).

polymerization takes place when any two of four proteins (ChSy-1, ChSy-2, ChSy-3 or ChPF) were co-expressed and the acceptor substrate was α-TM with a truncated linkage-region tetrasaccharide, GlcAβ1-3Galβ1-3Galβ1-4Xyl [3–5]. Therefore in the present study we measured polymerization activity using α-TM or [^{3}H]GalNAc-TM with the non-reducing terminal GalNAc-linkage pentasaccharide structure as an acceptor substrate and co-expression of any two of the ChSy-1, ChSy-2, ChSy-3 and ChPF proteins as the enzyme source (see the Experimental section). Polymerization did not occur with any enzyme subunit combination when [^{3}H]GalNAc-TM was the acceptor substrate (Figure 2, open squares). These results indicated that the non-reducing terminal GalNAc-linkage structure did not serve as a chondroitin polymerization substrate.

Involvement of ChGn-1 in increasing the number of CS chains

Previously, we found that overexpression of ChGn-1 slightly increases CS levels in L cells (see Table 2 in [26]). This result indicates that ChGn-1 might regulate the production of CS. Therefore we examined the effects of shRNA-mediated knockdown of ChGn-1 in L cells in the present study. The

efficiency of gene shRNA-mediated silencing was determined by quantitative real-time RT–PCR. Transfection with ChGn-1 shRNA (L-shRNA ChGn-1-1 and L-shRNA ChGn-1-2 cells: two different shRNAs targeted against *ChGn-1* were used) resulted in a 60–80 % reduction in steady-state *ChGn-1* mRNA and an 18–22 % decrease in CS when compared with control L cells (Table 1). These findings indicate that the knockdown of ChGn-1 decreases CS levels in L cells, corresponding to expression levels of ChGn-1 (Table 1).

We next compared the CS chain lengths in L-shRNA ChGn-1-1, L-shRNA ChGn-1-2, and mock-transfected L cells. Gel-filtration analysis using a Superdex™ 200 column revealed that the length of CS chains in L-shRNA ChGn-1-1- and L-shRNA ChGn-1-2-transfected cells was similar to that in mock-transfected cells (Figure 3). Thus both *in vitro* and *in vivo* studies have shown that ChGn-1 regulates the number of CS chains, in spite of the fact that chondroitin polymerization did not occur on the non-reducing terminal GalNAc-linkage structure.

Involvement of the GalNAc(4-*O*-sulfate)-linkage structure in chondroitin polymerization

We recently found that the non-reducing terminal 4-O-sulfation of GalNAc residues on the repeating disaccharide region synthesized by C4ST-1 and ChGn-2 facilitates the elongation of CS chains only by chondroitin polymerase consisting of ChSy-1 and ChPF [26]. On the basis of this result, we predicted that the non-reducing terminal 4-O-sulfation of newly synthesized GalNAc-linkage regions might promote the elongation of CS chains by chondroitin polymerases. We measured polymerization activity using [^{35}S]GalNAc(4S)-TM as acceptor substrates, and the co-expression of any combination of two ChSy-1, ChSy-2, ChSy-3 and ChPF as the enzyme source. Reaction products obtained were subjected to reductive β-elimination using NaBH$_4$/NaOH, and the radiolabelled saccharides released were analysed by gel-filtration chromatography using a Superdex™ 200 column. Chondroitin polymerization was induced on the [^{35}S]GalNAc(4S)-TM when any combination of protein subunits was used as the enzyme source (Figure 2, closed circles). Notably, the length of the chondroitin chains synthesized on [^{35}S]GalNAc(4S)-TM by ChSy-1–ChPF, ChSy-1–ChSy-3 or ChSy-3–ChPF, and on α-TM were comparable (Figures 2A, 2C and 2F), but the chondroitin chains polymerized on [^{35}S]GalNAc(4S)-TM by ChSy-1–ChSy-2, ChSy-2–ChPF or ChSy-2–ChSy-3 were longer than those formed on α-TM (Figures 2B, 2D and 2E). These results indicated that chondroitin polymerization was facilitated by the non-reducing terminal GalNAc(4-*O*-sulfate)-linkage structure. Thus multiple enzyme complexes, which each comprised any two of four ChSy family members, synthesized more CS chains when there was a non-reducing terminal GalNAc(4-*O*-sulfate)-linkage structure on the CS acceptor substrate.

Identification of sulfotransferases involved in the 4-O-sulfation of the GalNAc-linkage pentasaccharide

Reportedly, C4ST-1, C4ST-2 and D4ST-1 catalyse the transfer of sulfate from PAPS to position 4 of the internal GalNAc residue of chondroitin [14,15]. However, it is not clear whether C4ST-1, C4ST-2 or D4ST-1 is also responsible for transferring the sulfate to position 4 of the non-reducing terminal GalNAc-linkage residue. Hence, we examined whether C4ST-1, C4ST-2 and/or D4ST-1 could sulfate the GalNAc-linkage residue. For this analysis, the recombinant C4ST-1, C4ST-2 and D4ST-1 were expressed and initially evaluated for sulfotransferase activities towards internal GalNAc residues using polymer

Table 1   Disaccharide composition of CS in mock- and shChGn-1-transfected L cells

Values are expressed as pmol of disaccharide per mg of dried homogenate of the cells and are means $\pm$ S.E.M. for three determinations. ΔDi-0S, ΔHexA(α1-3)GalNAc; ΔDi-6S, ΔHexAα1-3GalNAc(6-O-sulfate); ΔDi-4S, ΔHexAα1-3GalNAc(4-O-sulfate); ΔDi-diS$_D$, ΔHexA(2-O-sulfate)α1-3GalNAc(6-O-sulfate); ΔDi-diS$_E$, ΔHexAα1-3GalNAc(4-O-sulfate,6-O-sulfate); N.D., not detected (<0.01 pmol/mg).

(a) Composition

Disaccharide	L-mock [pmol/mg (mol%)]	L-shRNA ChGn-1-1 [pmol/mg (mol%)]	L-shRNA ChGn-1-2 [pmol/mg (mol%)]
ΔDi-0S	34 $\pm$ 8 (5)	20 $\pm$ 1 (7)	14 $\pm$ 1 (6)
ΔDi-6S	4 $\pm$ 2 (1)	13 $\pm$ 1 (5)	11 $\pm$ 1 (4)
ΔDi-4S	251 $\pm$ 18 (76)	210 $\pm$ 16 (78)	199 $\pm$ 19 (77)
ΔDi-diS$_D$	N.D.	N.D.	N.D.
ΔDi-diS$_E$	39 $\pm$ 9 (12)	27 $\pm$ 4 (10)	34 $\pm$ 3 (13)
Total (pmol/mg)	328 $\pm$ 20	270 $\pm$ 22	258 $\pm$ 25

(b) Relative expression

Transcript	L-mock	L-shRNA ChGn-1-1	L-shRNA ChGn-1-2
Relative expression of *ChGn-1**	1.0	0.4	0.2
Relative expression of *ChGn-2*	1.0	1.0	1.2
Relative expression of *C4ST-1*	1.0	0.9	1.1
Relative expression of *C4ST-2*	1.0	1.1	1.3

*Relative amounts of the *ChGn-1* transcript were quantified by quantitative real-time RT–PCR. *ChGn-1* mRNA expression values were normalized to *GAPDH* mRNA levels and are given relative to those in L cells.

Table 2   Disaccharide composition of CS in mock-, C4ST-2- and shC4ST-2-transfected L cells

Values are expressed as pmol of disaccharide per mg of dried homogenate of the cells and are means $\pm$ S.E.M. for three determinations. ΔDi-0S, ΔHexA(α1-3)GalNAc; ΔDi-6S, ΔHexAα1-3GalNAc(6-O-sulfate); ΔDi-4S, ΔHexAα1-3GalNAc(4-O-sulfate); ΔDi-diS$_D$, ΔHexA(2-O-sulfate)α1-3GalNAc(6-O-sulfate); ΔDi-diS$_E$, ΔHexAα1-3GalNAc(4-O-sulfate,6-O-sulfate); N.D., not detected (<0.01 pmol/mg).

(a) Composition

Disaccharide	L-mock [pmol/mg (mol%)]	L-C4ST-2-1 [pmol/mg (mol%)]	L-C4ST-2-2 [pmol/mg (mol%)]	L-shRNA C4ST-2-1 [pmol/mg (mol%)]	L-shRNA C4ST-2-2 [pmol/mg (mol%)]
ΔDi-0S	54 $\pm$ 6 (15)	110 $\pm$ 7 (16)	85 $\pm$ 4 (15)	47 $\pm$ 1 (20)	33 $\pm$ 4 (17)
ΔDi-6S	6 $\pm$ 2 (2)	11 $\pm$ 5 (2)	31 $\pm$ 3 (5)	7 $\pm$ 1 (3)	3 $\pm$ 1 (2)
ΔDi-4S	250 $\pm$ 20 (70)	472 $\pm$ 23 (69)	393 $\pm$ 7 (69)	150 $\pm$ 2 (63)	132 $\pm$ 19 (69)
ΔDi-diS$_D$	N.D.	N.D.	N.D.	N.D.	N.D.
ΔDi-diS$_E$	48 $\pm$ 12 (13)	89 $\pm$ 6 (13)	60 $\pm$ 4 (11)	35 $\pm$ 4 (15)	22 $\pm$ 3 (12)
Total (pmol/mg)	358 $\pm$ 8	682 $\pm$ 19	569 $\pm$ 12	239 $\pm$ 6	190 $\pm$ 25

(b) Relative expression

Transcript	L-mock	L-C4ST-2-1	L-C4ST-2-2	L-shRNA C4ST-2-1	L-shRNA C4ST-2-2
Relative expression of *C4ST-2**	1.0	7.6	3.4	0.3	0.2
Relative expression of *C4ST-1*	1.0	0.8	1.2	0.8	1.0
Relative expression of *ChGn-1*	1.0	0.9	0.9	1.1	1.0
Relative expression of *ChGn-2*	1.0	1.0	1.0	1.0	1.2

*Relative amounts of the *C4ST-2* transcript were quantified by quantitative real-time RT–PCR. *C4ST-2* mRNA expression values were normalized to *GAPDH* mRNA levels and are given relative to those in L cells.

chondroitin as an acceptor [15]. The activity of C4ST-1, C4ST-2 or D4ST-1 was 550, 81 or 89 pmol/μg per h respectively. Then, sulfotransferase activity was determined using GalNAc-TM as the acceptor substrate and [^{35}S]PAPS as the donor substrate. C4ST-2 transferred sulfate to GalNAc-TM much more efficiently than did C4ST-1 (Figure 4A). D4ST-1 showed no activity when GalNAc-TM was used as an acceptor (Figure 4A, open triangles, inset). To identify the ^{35}S-labelled products synthesized on the GalNAc-linkage pentasaccharide of α-TM, the products were subjected to reductive β-elimination and then digested to completion with chondroitinase AC-II, which cleaves the β1-4-N-acetylgalactosaminidic linkage. The digests were separated by gel-filtration chromatography using a Superdex™

peptide column, and a large peak was detected at the position corresponding to GalNAc-4-O-SO$_4$ (Figure 4B, closed circles). In sharp contrast, C4ST-1 transferred sulfate to the GalNAc residues and to a Gal residue of the linkage region, albeit transfer to the linkage region was much less efficient (Figure 4B, open circles, inset). These results indicated that C4ST-2 efficiently and selectively transferred sulfate from PAPS to the non-reducing terminal GalNAc-linkage residue.

Introduction of ChGn-1 to sog9 cells

Previously we found that C4ST-1 regulates the 4-O-sulfation of CS and the length and amount of CS chains [23], and that,
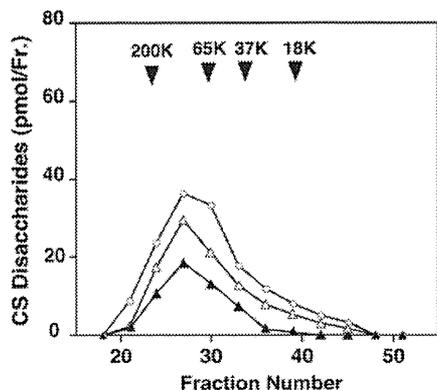
Figure 3   Analysis of the length of CS chains from L, L-shRNA ChGn-1-1 and L-shRNA ChGn-1-2 cells

Purified CS fractions were subjected to reductive β-elimination using NaBH$_4$/NaOH and then analysed by gel-filtration chromatography on a Superdex™ 200 column (10 mm×300 mm). The digests of individual fractions obtained with chondroitinase ABC were derivatized with 2-aminobenzamide and then analysed by HPLC. The amounts of the 2-aminobenzamide derivatives of unsaturated disaccharides were calculated based on fluorescence intensity. Samples from L-shRNA ChGn-1-1 ($\triangle$), L-shRNA ChGn-1-2 ($\blacktriangle$) and mock-transfected L ($\bigcirc$) cells are shown. Arrowheads indicate the size of molecular mass standards in kDa. Data represent one of a series of three independent experiments, where all three experiments gave essentially the same results.
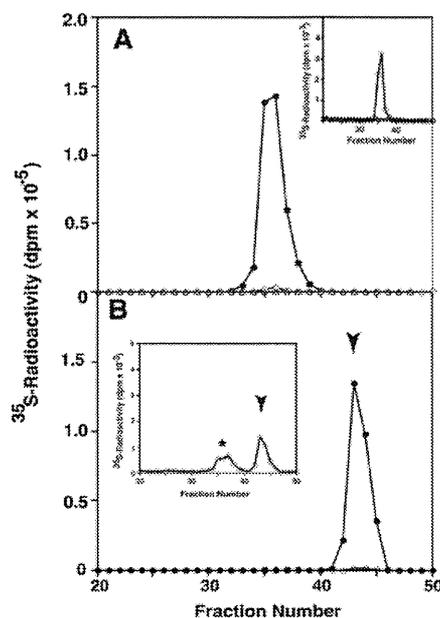
Figure 4   Identification of ^{35}S-labelled sulfotransferase reaction products prepared using C4ST-1, C4ST-2 and D4ST-1 as the enzyme sources

(**A**) GalNAcβ1-4GlcAβ1-3Galβ1-3Galβ1-4Xylβ1-O-TM was tested as a potential acceptor for sulfotransferase reactions, where C4ST-1 ($\bigcirc$), C4ST-2 ($\bullet$) or D4ST-1 ($\triangle$) was used as an enzyme source, as described in the Experimental section. ^{35}S-Labelled sulfotransferase reaction products were first isolated by gel filtration, subjected to reductive β-elimination using NaBH$_4$/NaOH, and then rechromatographed on a Superdex™ peptide column with 0.25 M NH$_4$HCO$_3$/7 % propan-1-ol as the eluent. The inset shows a different scaling when C4ST-1 ($\bigcirc$) or D4ST-1 ($\triangle$) was used as an enzyme source. (**B**) ^{35}S-Labelled sulfotransferase reaction products were digested with chondroitinase AC-II. The chondroitinase AC-II digests derived from reaction products using C4ST-1 ($\bigcirc$) or C4ST-2 ($\bullet$) were isolated by gel filtration on a Superdex™ peptide column using 0.25 M NH$_4$HCO$_3$/7 % propan-1-ol as the eluent. The inset shows a different scaling when C4ST-1 ($\bigcirc$) was used as an enzyme source. The arrowhead indicates the elution position of GalNAc-4-SO$_4$. The peaks marked by an asterisk indicate the elution position of GlcAβ-Gal(4-O-sulfate)-Gal-Xyl-ol.
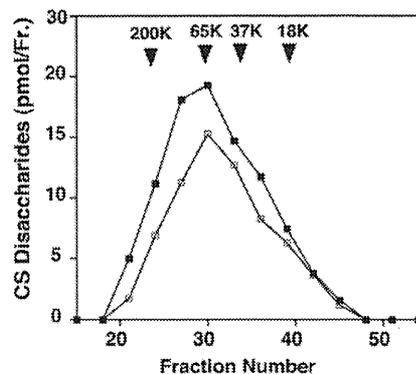

Figure 5   Analysis of the length of CS chains in sog9 and sog9-ChGn-1-1 cells

Purified CS fractions were subjected to reductive β-elimination using NaBH$_4$/NaOH and then analysed by gel-filtration chromatography on a Superdex™ 200 column (10 mm×300 mm). The digests of individual fractions obtained with chondroitinase ABC were derivatized with 2-aminobenzamide and then analysed by HPLC. The amounts of the 2-aminobenzamide derivatives of unsaturated disaccharides were calculated based on fluorescence intensity. Samples from sog9-ChGn-1-1 ($\blacksquare$) and mock-transfected sog9 ($\square$) cells are shown. Arrowheads indicate the size of molecular mass standards in kDa. Data represent one of a series of three independent experiments, and all three experiments gave essentially the same results.

however, overexpression of ChGn-1 increases CS levels in C4ST-1-deficient sog9 cells (see sog9-ChGn-1-1 and sog9-ChGn-1-2 cells in Table 3 in [26]). To further assess whether C4ST-1 was dispensable for regulating the number of CS chains synthesized by ChGn-1, the lengths of CS chains in sog9-ChGn-1-1-transfected and mock-transfected sog9 cells were compared. Gel-filtration analysis using a Superdex™ 200 column revealed that the length of CS chains in sog9-ChGn-1-1 cells was similar to that in mock-transfected cells (Figure 5). These results indicated that ChGn-1 regulated the number of CS chains without C4ST-1, and that C4ST-2 might play a key role in controlling the number of CS moieties synthesized by ChGn-1.

Introduction of C4ST-2 into L cells

We next examined whether C4ST-2 regulates the number of CS chains by preparing L cells in which C4ST-2 is overexpressed. The amount and disaccharide composition of CS isolated from two stable L cell clones that express different levels of C4ST-2 (high expression L-C4ST-2-1 and low expression L-C4ST-2-2 cells) were analysed by HPLC (Table 2). Although the disaccharide compositions of CS found in L-C4ST-2-1 and L-C4ST-2-2 cells were similar to those in control L cells, the levels of CS were higher in L-C4ST-2-1 and L-C4ST-2-2 cells; moreover, the CS levels corresponded to the C4ST-2 expression levels (Table 2).

We then determined whether knockdown of C4ST-2 decreased the amount of CS in L cells. The efficiency of gene silencing was determined by quantitative RT–PCR. Transfection with C4ST-2 shRNA (L-shRNA C4ST-2-1 or L-shRNA C4ST-2-2 cells: two different shRNAs targeted against C4ST-2 were used) resulted in a 70–80 % knockdown of *C4ST-2* mRNA and a 33–47 % decrease in the amount of CS when compared with control L cells. These results indicated that C4ST-2 regulated CS levels, and that CS levels were proportional to *C4ST-2* expression levels (Table 2).

Involvement of C4ST-2 in the increased number of CS chains

We next compared the lengths of CS chains in L-C4ST-2-1-, L-C4ST-2-2-, L-shRNA C4ST-2-1-, L-shRNA C4ST-2-2- and mock-transfected L cells. Gel-filtration analysis using a
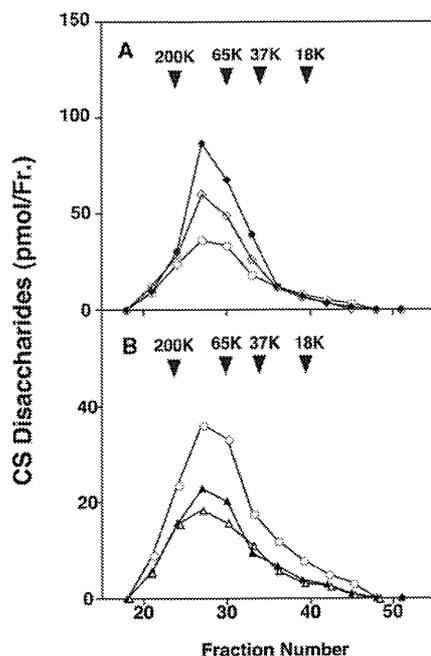
Figure 6 Analysis of the length of CS chains in L, L-C4ST-2, L-shRNA C4ST-2-1 and L-shRNA C4ST-2-2 cells

Purified CS fractions were subjected to reductive β-elimination using NaBH$_4$/NaOH and then analysed by gel-filtration chromatography on a Superdex^{TM} 200 column (10 mm×300 mm). The digests of individual fractions obtained with chondroitinase ABC were derivatized with 2-aminobenzamide and then analysed by HPLC. The amounts of the 2-aminobenzamide derivatives of unsaturated disaccharides were calculated based on fluorescence intensity. (**A**) The samples from L-C4ST-2-1 (◆), L-C4ST-2-2 (◇) and mock-transfected L (○) cells are shown. (**B**) The samples from L-shRNA C4ST-2-1 (▲), L-shRNA C4ST-2-2 (△) and mock-transfected L (○) cells are shown. Arrowheads indicate the size of the molecular standards in kDa. Data represent one of a series of three independent experiments, and all three experiments gave essentially the same results.

Superdex^{TM} 200 column revealed that the CS chain lengths in cells transfected with L-C4ST-2-1, L-C4ST-2-2, L-shRNA C4ST-2-1 or L-shRNA C4ST-2-2 were comparable with those in control L cells (Figures 6A and 6B), indicating that C4ST-2 regulated only the number of CS chains in L cells and that the number of CS chains corresponded to *C4ST-2* expression levels.

DISCUSSION

Previously, we have demonstrated that co-expression of any two of four ChSy family members, ChSy-1, ChSy-2, ChSy-3 and ChPF, promoted chondroitin polymerization with alternating GalNAc and GlcA residues on the linkage-region tetrasaccharide of α-TM [3–5]. These results indicated that ChGn-1 and ChGn-2, both of which have GalNAcT activity, were not required for chondroitin polymerization on the linkage-region tetrasaccharide. In fact, our recent studies found that knockdown of ChGn-2 resulted in a decrease in CS chain length and that ChGn-2 was involved in CS chain elongation [26]. In contrast with ChGn-2, ChGn-1-deficient mice had fewer CS chains in developing cartilage and a delayed cartilage development [20]. These results suggest that ChGn-1 is required for efficient initiation of CS chain polymerization; moreover, the presence of chondroitin polymerase, meaning any two of ChSy-1, ChSy-2, ChSy-3 and ChPF, does not compensate for the loss of ChGn-1. In addition, the number of CS chains on

specific core proteins may be tightly regulated during cartilage development by temporal and spatial regulation of ChGn-1 expression, and progression of cartilage disease may result from defects in these regulatory systems.

Sakai et al. [27] reported that *in vitro* overexpression of ChGn-1 in chondrosarcoma cells increased the number of CS chains. Their observations, like ours, indicate that ChGn-1 regulates the initiation of CS. Nevertheless, the results of the present study indicated that chondroitin polymerization did not occur on the non-reducing terminal GalNAc-linkage structure (Figure 2, open squares). Interestingly, the non-reducing terminal GalNAc(4-*O*-sulfate)-linkage structure of CS was associated with an increased number of CS chains when the enzyme source was any one of several complexes that comprised any two of the four ChSy family (Figure 2). In addition, C4ST-2 efficiently transferred sulfate to the non-reducing terminal GalNAc-linkage residue (Figure 4). In conjunction with our previous findings, these results indicate that ChGn-1 co-operates with C4ST-2 to increase the number of CS moieties.

Notably, on the basis of the data in Figure 2, ChSy-1–ChSy-3 enzyme complexes seemed to play a central role in chondroitin polymerization on α-TM, although every ChSy complex tested polymerized chondroitin on α-TM. In our previous study, ChSy family members co-expressed in various combinations exhibited distinct but overlapping acceptor substrate specificities with two synthetic acceptor substrates, GlcAβ1-3Galβ1-*O*-naphthalenemethanol and GlcAβ1-3Galβ1-*O*-C$_2$H$_4$NH-benzyloxycarbonyl, both of which share a disaccharide sequence with the GAG–protein linkage region tetrasaccharide [4]. When using the two synthetic acceptor substrates, two complexes, ChSy-1–ChPF and ChSy-1–ChSy-3, polymerized more chondroitin than other complexes [4]. Moreover, we recently found that the non-reducing terminal 4-O-sulfation of GalNAc residues synthesized by C4ST-1 and ChGn-2 facilitated the elongation of CS chains only when the chondroitin polymerase comprised ChSy-1 and ChPF, and no polymerization was induced on these acceptors when ChSy-1 and ChSy-2, ChSy-1 and ChSy-3, ChSy-2 and ChSy-3, ChSy-2 and ChPF, or ChSy-3 and ChPF were co-expressed [26]. Furthermore, as shown in the present study, the non-reducing terminal GalNAc(4-*O*-sulfate)-linkage structure of CS was associated with an increase in the number of CS chains when any one of six ChSy complexes was the polymerase (Figure 2). Thus each ChSy complex may play a specific role in the biosynthesis of CS.

In the present study we propose that the chondroitin backbone was synthesized via two pathways (Figure 7). Pathway A shows that after synthesis of the linkage-region tetrasaccharide, the ChSy-1–ChSy-3 complex is primarily responsible for chondroitin polymerization. Pathway B shows that following complete synthesis of the linkage-region tetrasaccharide, ChGn-1 catalyses the transfer of a single GalNAc residue to the tetrasaccharide-linkage region and C4ST-2 then mediates the 4-O-sulfation of the non-reducing terminal GalNAc residue. Finally, the non-reducing terminal 4-O-sulfation of the GalNAc-linkage structure facilitated the elongation of CS chains via chondroitin polymerases that comprised any combination of two ChSy family members, although the chain lengths of chondroitin synthesized by different ChSy enzyme complexes differed (Figure 2). These results indicated that the mechanism of CS chain initiation, which is largely mediated by the ChGn-1 and C4ST-2, were similar to, but distinct from, the mechanisms of chain elongation, which was largely mediated by ChGn-2 and C4ST-1 [26].

In a previous study, it was shown that the synthesis of abnormally long CS chains that occurs during the development of atherosclerosis is accompanied by increases in expression
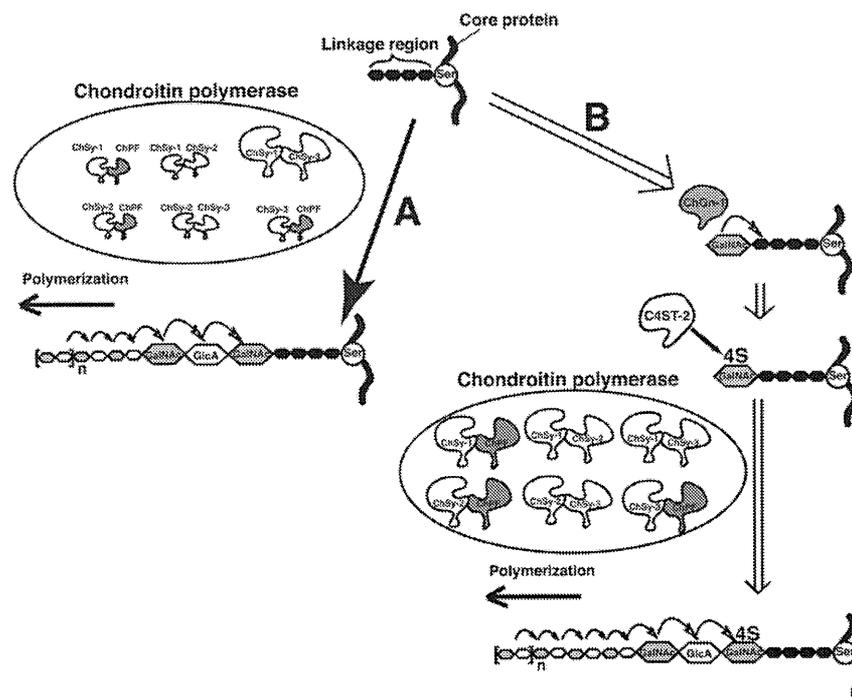
Figure 7   Mechanisms that increase the number of CS chains

CS is synthesized via two pathways. (**A**) Following complete synthesis of the linkage-region tetrasaccharide, chondroitin polymerization with alternating GalNAc and GlcA residues occurs by an enzyme complex comprising any two of four proteins: ChSy-1, ChSy-2, ChSy-3 and ChPF. (**B**) Following complete synthesis of the linkage-region tetrasaccharide, a single GalNAc residue is transferred to the tetrasaccharide-linkage region by ChGn-1, and C4ST-2 catalyses the 4-O-sulfation of the non-reducing terminal GalNAc residue. Finally, the non-reducing terminal 4-O-sulfation of the GalNAc-linkage structure facilitates the elongation of CS chains, which is catalysed by chondroitin polymerase consisting of any two of the following four proteins: ChSy-1, ChSy-2, ChSy-3 and ChPF.

of C4ST-1 and ChGn-2 [28]. In contrast, C4ST-2 and ChGn-1 expression levels do not change during the progression of atherosclerosis, suggesting that C4ST-2 and ChGn-1 may not be involved in CS chain elongation during the development of atherosclerosis [28]. These results indicate that functions of ChGn-1 and ChGn-2, or C4ST-1 and C4ST-2, are different, despite their overlapping substrate specificities *in vitro*. In addition, the C4ST-1–ChGn-2 and C4ST-2–ChGn-1 complexes are important in the regulation of CS chain length and the number of CS chains respectively. An analysis of ChGn-2- or C4ST-2-knockout mice should provide further insight into the distinct functions of these proteins. C4ST-2-knockout mice may exhibit a similar phenotype to ChGn-1-knockout mice.

ChGn-1-knockout mice had less cartilage than wild-type mice. Sato et al. [29] also indicated that ChGn-1-deficient mice exhibited slight dwarfism due to a minor impairment of endochondral ossification. These results suggest that ChGn-1 is required for normal cartilage development. To date, many of these cartilage deficiencies are characteristic of the degenerative alterations observed with OA (osteoarthritis). OA is a degenerative disease characterized by a loss of matrix CS and cartilage integrity [30]. A genome-wide gene expression analysis that compared human OA cartilage with normal donor cartilage identified an altered level of C4ST-1 expression in OA cartilage [31]. In fact, C4ST-1-knockout mice have severe cartilage defects, and are characterized by disorganized and hypercellular cartilage growth plates with a fibrillated ECM (extracellular matrix) and an overall loss of CS [32]. On the basis of the findings that both C4ST-1 and ChGn-1 play key roles in mammalian chondrocyte development and in the maintenance of healthy cartilage, it is

likely that abnormal ChGn-1 and C4ST-2 expression may be involved in the pathogenic mechanisms of OA.

More recently, we found two missense mutations in the *ChGn-1* gene, and both were associated with a profound decrease in enzyme activity in two patients with neuropathy [33]. As we found in the present study, ChGn-1 regulated the chain number and amount of CS in these patients, which indicates that patients with neuropathies may suffer from decreased levels of CS. In addition, we demonstrated that ChGn-1 co-operates with C4ST-2 to increase the number of CS moieties. Thus C4ST-2 may also be associated with the pathogenesis of peripheral neuropathies because C4ST-2 abnormalities may inhibit recovery from minor trauma. Studies on larger numbers of patients and complete family studies are in progress.

AUTHOR CONTRIBUTION

ACKNOWLEDGEMENT

FUNDING

REFERENCES

1 Sugahara, K. and Kitagawa, H. (2000) Recent advances in the study of the biosynthesis and functions of sulfated glycosaminoglycans. Curr. Opin. Struct. Biol. **10**, 518–527

2 Kitagawa, H., Uyama, T. and Sugahara, K. (2001) Molecular cloning and expression of a human chondroitin synthase. J. Biol. Chem. **276**, 38721–38726

3 Izumikawa, T., Uyama, T., Okuura, Y., Sugahara, K. and Kitagawa, H. (2007) Involvement of chondroitin sulfate synthase-3 (chondroitin synthase-2) in chondroitin polymerization through its interaction with chondroitin synthase-1 or chondroitin polymerizing factor. Biochem. J. **403**, 545–552

4 Izumikawa, T., Koike, T., Shiozawa, S., Sugahara, K., Tamura, J. and Kitagawa, H. (2008) Identification of chondroitin sulfate glucuronyltransferase as chondroitin synthase-3 involved in chondroitin polymerization: chondroitin polymerization is achieved by multiple enzyme complexes consisting of chondroitin synthase family members. J. Biol. Chem. **283**, 11396–11406

5 Kitagawa, H., Izumikawa, T., Uyama, T. and Sugahara, K. (2003) Molecular cloning of a chondroitin polymerizing factor that cooperates with chondroitin synthase for chondroitin polymerization. J. Biol. Chem. **278**, 23666–23671

6 Uyama, T., Kitagawa, H., Tamura, J. and Sugahara, K. (2002) Molecular cloning and expression of human chondroitin N-acetylgalactosaminyltransferase: the key enzyme for chain initiation and elongation of chondroitin/dermatan sulfate on the protein linkage region tetrasaccharide shared by heparin/heparan sulfate. J. Biol. Chem. **277**, 8841–8846

7 Gotoh, M., Sato, T., Akashima, T., Iwasaki, H., Kameyama, A., Mochizuki, H., Yada, T., Inaba, N., Zhang, Y., Kikuchi, N. et al. (2002) Enzymatic synthesis of chondroitin with a novel chondroitin sulfate N-acetylgalactosaminyltransferase that transfers N-acetylgalactosamine to glucuronic acid in initiation and elongation of chondroitin sulfate synthesis. J. Biol. Chem. **277**, 38189–38196

8 Sato, T., Gotoh, M., Kiyohara, K., Akashima, T., Iwasaki, H., Kameyama, A., Mochizuki, H., Yada, T., Inaba, N., Togayachi, A. et al. (2003) Differential roles of two N-acetylgalactosaminyltransferases, CSGalNAcT-1, and a novel enzyme, CSGalNAcT-2. Initiation and elongation in synthesis of chondroitin sulfate. J. Biol. Chem. **278**, 3063–3071

9 Uyama, T., Kitagawa, H., Tanaka, J., Tamura, J., Ogawa, T. and Sugahara, K. (2003) Molecular cloning and expression of a second chondroitin N-acetylgalactosaminyltransferase involved in the initiation and elongation of chondroitin/dermatan sulfate. J. Biol. Chem. **278**, 3072–3078

10 Kusche-Gullberg, M. and Kjellén, L. (2003) Sulfotransferases in glycosaminoglycan biosynthesis. Curr. Opin. Struct. Biol. **13**, 605–611

11 Hiraoka, N., Nakagawa, H., Ong, E., Akama, T. O., Fukuda, M. N. and Fukuda, M. (2000) Molecular cloning and expression of two distinct human chondroitin 4-O-sulfotransferases that belong to the HNK-1 sulfotransferase gene family. J. Biol. Chem. **275**, 20188–20196

12 Kang, H.-G., Evers, M. R., Xia, G., Baenziger, J. U. and Schachner, M. (2002) Molecular cloning and characterization of chondroitin-4-O-sulfotransferase-3: a novel member of the HNK-1 family of sulfotransferases. J. Biol. Chem. **277**, 34766–34772

13 Evers, M. R., Xia, G., Kang, H.-G., Schachner, M. and Baenziger, J. U. (2001) Molecular cloning and characterization of a dermatan-specific N-acetylgalactosamine 4-O-sulfotransferase. J. Biol. Chem. **276**, 36344–36354

14 Yamauchi, S., Mita, S., Matsubara, T., Fukuta, M., Habuchi, H., Kimata, K. and Habuchi, O. (2000) Molecular cloning and expression of chondroitin 4-sulfotransferase. J. Biol. Chem. **275**, 8975–8981

15 Mikami, T., Mizumoto, S., Kago, N., Kitagawa, H. and Sugahara, K. (2003) Specificities of three distinct human chondroitin/dermatan N-acetylgalactosamine 4-O-sulfotransferases demonstrated using partially desulfated dermatan sulfate as an acceptor: implication of differential roles in dermatan sulfate biosynthesis. J. Biol. Chem. **278**, 36115–36127

16 Fukuta, M., Uchimura, K., Nakashima, K., Kato, M., Kimata, K., Shinomura, T. and Habuchi, O. (1995) Molecular cloning and expression of chick chondrocyte chondroitin 6-sulfotransferase. J. Biol. Chem. **270**, 18575–18580

17 Tsutsumi, K., Shimakawa, H., Kitagawa, H. and Sugahara, K. (1998) Functional expression and genomic structure of human chondroitin 6-sulfotransferase. FEBS Lett. **441**, 235–241

18 Kobayashi, M., Sugumaran, G., Liu, J., Shworak, N. W., Silbert, J. E. and Rosenberg, R. D. (1999) Molecular cloning and characterization of a human uronyl 2-sulfotransferase that sulfates iduronyl and glucuronyl residues in dermatan/chondroitin sulfate. J. Biol. Chem. **274**, 10474–10480

19 Ohtake, S., Ito, Y., Fukuta, M. and Habuchi, O. (2001) Functional expression and genomic structure of human chondroitin 6-sulfotransferase. J. Biol. Chem. **276**, 43894–43900

20 Watanabe, Y., Takeuchi, K., Higa-Onaga, S., Tsujita, M., Abe, M., Natsume, R., Li, M., Furuichi, T., Saeki, M., Izumikawa, T. et al. (2010) Chondoroitin sulfate N-acetylgalactosaminyltransferase-1 is required for normal cartilage development. Biochem. J. **432**, 47–55

21 Nawa, K., Sakano, K., Fujiwara, H., Sato, Y., Sugiyama, N., Teruuchi, T., Iwamoto, M. and Marumoto, Y. (1990) Presence and function of chondroitin-4-sulfate on recombinant human soluble thrombomodulin. Biochem. Biophys. Res. Commun. **171**, 729–737

22 Nadanaka, S., Kitagawa, H. and Sugahara, K. (1998) Demonstration of the immature glycosaminoglycan tetrasaccharide sequence GlcAβ1-3Galβ1-3Galβ1-4Xyl on recombinant soluble human α-thrombomodulin. An oligosaccharide structure on a 'part-time' proteoglycan. J. Biol. Chem. **273**, 33728–33734

23 Uyama, T., Ishida, M., Izumikawa, T., Trybala, E., Tufaro, F., Bergström, T., Sugahara, K. and Kitagawa, H. (2006) Chondroitin 4-O-sulfotransferase-1 regulates E disaccharide expression of chondroitin sulfate required for herpes simplex virus infectivity. J. Biol. Chem. **281**, 38668–38674

24 Kinoshita, A. and Sugahara, K. (1999) High-performance liquid chromatography: application to disaccharide composition analysis and exosequencing of oligosaccharides. Anal. Biochem. **269**, 367–378

25 Koike, T., Izumikawa, T., Tamura, J. and Kitagawa, H. (2009) FAM20B is a kinase that phosphorylates xylose in the glycosaminoglycan-protein linkage region. Biochem. J. **421**, 157–162

26 Izumikawa, T., Okuura, Y., Koike, T., Sakoda, N. and Kitagawa, H. (2011) Chondroitin 4-O-sulfotransferase-1 regulates the chain length of chondroitin sulfate in co-operation with chondroitin N-acetylgalactosaminyltransferase-2. Biochem. J. **434**, 321–331

27 Sakai, K., Kimata, K., Sato, T., Gotoh, M., Narimatsu, H., Shinomiya, K. and Watanabe, H. (2007) Chondroitin sulfate N-acetylgalactosaminyltransferase-1 plays a critical role in chondroitin sulfate synthesis in cartilage. J. Biol. Chem. **282**, 4152–4161

28 Anggraeni, V. Y., Emoto, N., Yagi, K., Mayasari, D. S., Nakayama, K., Izumikawa, T., Kitagawa, H. and Hirata, K. (2011) Correlation of C4ST-1 and ChGn-2 expression with chondroitin sulfate chain elongation in atherosclerosis. Biochem Biophys. Res. Commun. **406**, 36–41

29 Sato, T., Kudo, T., Ikehara, Y., Ogawa, H., Hirano, T., Kiyohara, K., Hagiwara, K., Togayachi, A., Ema, M., Takahashi, S. et al. (2011) Chondroitin sulfate N-acetylgalactosaminyltransferase 1 is necessary for normal endochondral ossification and aggrecan metabolism. J. Biol. Chem. **286**, 5803–5812

30 Krasnokutsky, S., Samuels, J. and Abramson, S. B. (2007) Osteoarthritis in 2007. Bull. NYU. Hosp. Jt. Dis. **65**, 222–228

31 Karlsson, C., Dehne, T., Lindahl, A., Brittberg, M., Pruss, A. and Sittinger, M. (2010) Genome-wide expression profiling reveals new candidate genes associated with osteoarthritis. Osteoarthritis Cartilage **18**, 581–592

32 Kluppel, M., Wight, T. N., Chan, C., Hinek, A. and Wrana, J. L. (2005) Maintenance of chondroitin sulfation balance by chondroitin-4-sulfotransferase 1 is required for chondrocyte development and growth factor signaling during cartilage morphogenesis. Development **132**, 3989–4003

33 Saigoh, K., Izumikawa, T., Koike, T., Shimizu, J., Kitagawa, H. and Kusunoki, S. (2011) Chondroitin β1,4-N-acetylgalactosaminyltransferase-1 missense mutations are associated with neuropathies. J. Hum. Genet. **56**, 143–146
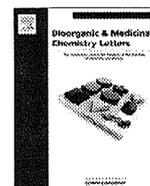
Synthesis and interaction with midkine of biotinylated chondroitin sulfate tetrasaccharides

Jun-ichi Tamura [a,*], Nao Tsutsumishita-Nakai [a], Yasuhiro Nakao [a], Manami Kawano [a], Saki Kato [a], Naoko Takeda [a], Satomi Nadanaka [b], Hiroshi Kitagawa [b]

[a] Department of Regional Environment, Tottori University, Tottori 680-8551, Japan
[b] Department of Biochemistry, Kobe Pharmaceutical University, Higashinada-ku, Kobe 658-8558, Japan

ARTICLE INFO

ABSTRACT

Regiospecifically sulfated chondroitin sulfate repeating tetrasaccharides, CS-OO, GlcAβ-GalNAcβ-GlcAβ-GalNAcβ;CS-EE, GlcAβ-GalNAc(4S6S)β-GlcAβ-GalNAc(4S6S)β; and CS-AA, GlcAβ-GalNAc(4S)β-GlcAβ-GalNAc(4S)β, having biotin linked with a hydrophilic linker at the reducing terminal were synthesized effectively by a coupling of the corresponding disaccharide units and regioselective sulfation. CS-EE showed greater affinity for midkine than CS-AA and CS-OO.

© 2011 Elsevier Ltd. All rights reserved.

Chondroitin sulfates (CSs) play pivotal roles in neuronal growth control,[1,2] lymphocyte homing,[3] viral infections[4] and cancer metastasis.[5] These biological processes are caused by interaction between CSs and characteristic proteins. It is known that regiospecific sulfate groups on glycans are involved in these interactions. It was also revealed that midkine interacted with GlcAβ-GalNAc(4S6S)β-type CS, though only naturally occurring oligosaccharides were employed in the experiments.[6] It is difficult to achieve accurate results with natural substrates because of incomplete homogeneity especially in relation to sulfation patterns.[2] We have been synthesizing CS repeating oligosaccharides of different lengths.[7–9] This Letter

describes the facile synthesis of CS repeating tetrasaccharides; CS-OO, GlcAβ-GalNAcβ-GlcAβ-GalNAcβ (**1**); CS-EE, GlcAβ-GalNAc(4S6S)β-GlcAβ-GalNAc(4S6S)β (**2**); and CS-AA, GlcAβ-GalNAc(4S)β-GlcAβ-GalNAc(4S)β (**3**) (Fig. 1), having biotin attached with a hydrophilic linker at the reducing terminal in order to clarify the effect of the microenvironment on glycans in protein–carbohydrate interactions. Jacquinet and his co-workers have just reported the synthesis of biotinylated CS oligosaccharides but with GalNAc-GlcA type sequences having a hydrophobic linker.[10,11] We investigated the interaction of midkine with the synthesized substrates (**1–3**) immobilized on plates for the first time.
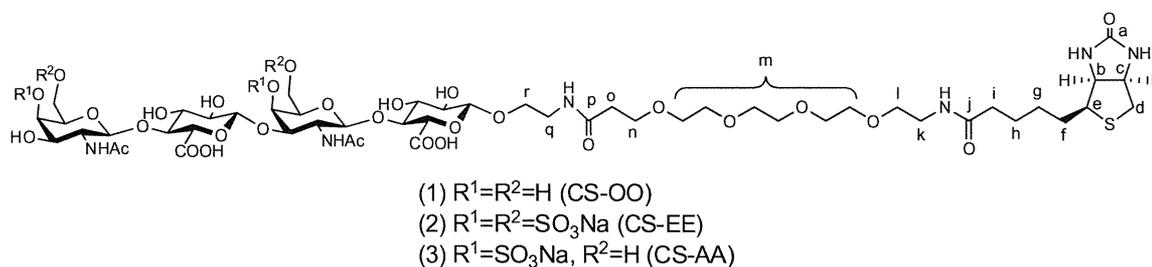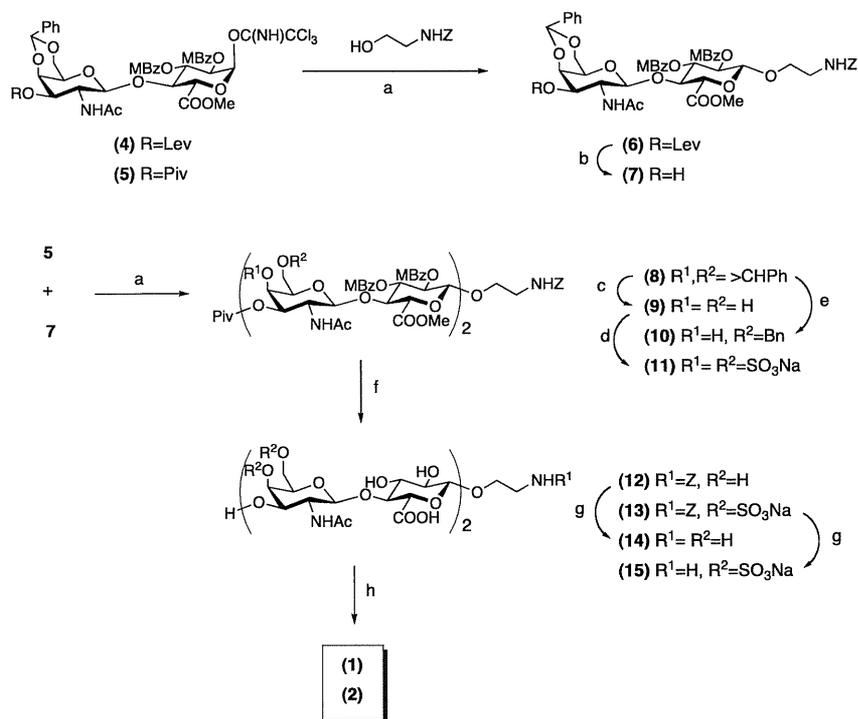

(1) R[1]=R[2]=H (CS-OO)
(2) R[1]=R[2]=SO₃Na (CS-EE)
(3) R[1]=SO₃Na, R[2]=H (CS-AA)

**Figure 1.** Target compounds (**1–3**).

* Corresponding author.
E-mail address: jtamura@rstu.jp (J. Tamura).

Scheme 1. Synthesis of **1** and **2**. Reagents and conditions: (a) TMSOTf, MSAW300, CH_2Cl_2, −20 °C to rt, 65% (for **6**), 58% (for **8**); (b) H_2NNH_2·AcOH, toluene–EtOH, 77%; (c) camphorsulfonic acid, CH_2Cl_2–MeOH, quant.; (d)SO_3·NMe_3, DMF, 60 °C, 86%; (e)BH_3·NMe_3, $AlCl_3$, MS4A, CH_2Cl_2–Et_2O, 13%; (f) aq LiOH, THF, then aq NaOH, CH_2Cl_2–MeOH, quant. (for **14**), 97% (for **15**); (g) H_2, Pd–C, cat. AcOH, aq EtOH; (h) NHS–PEO_4–biotin, 0.1 M Na_3PO_4, 0.15 M NaCl, 93% (for **1**), 69% (for **2**).
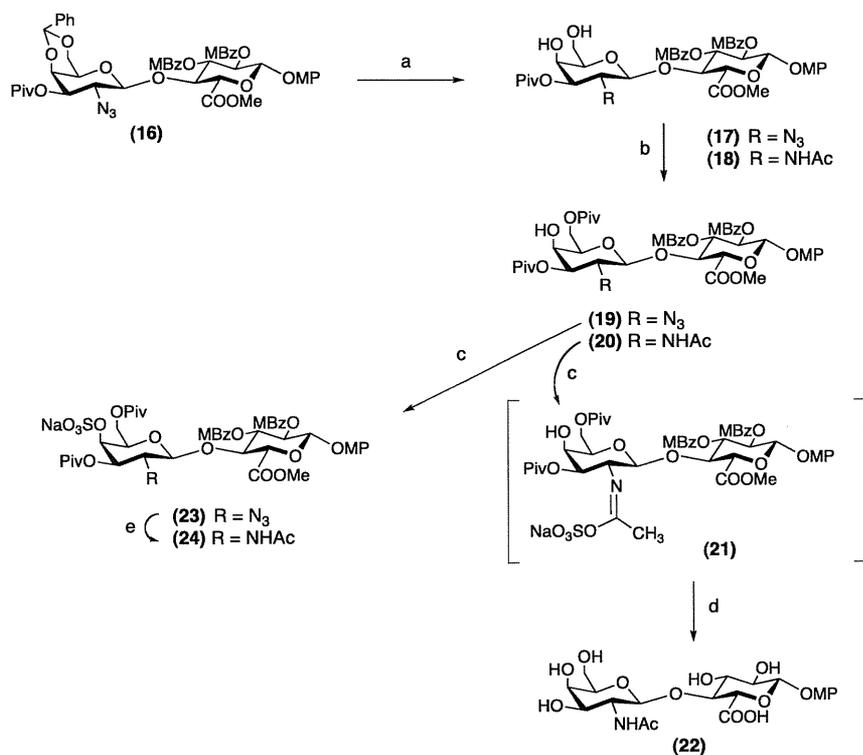
Scheme 2. Sulfation at *O*-4 of $GalN_3$ and GalNAc. Reagents and conditions: (a) camphorsulfonic acid, CH_2Cl_2–MeOH, 78%; (b) PivCl, pyridine, quant. (−40 °C, for **19**), 73% (rt, for **20**); (c)SO_3·NMe_3, DMF, 60 °C, 92% (for **21**), 96% (for **23**); (d)aq LiOH, THF, then aq NaOH, CH_2Cl_2–MeOH, 59%; (e) AcSH, 90%.
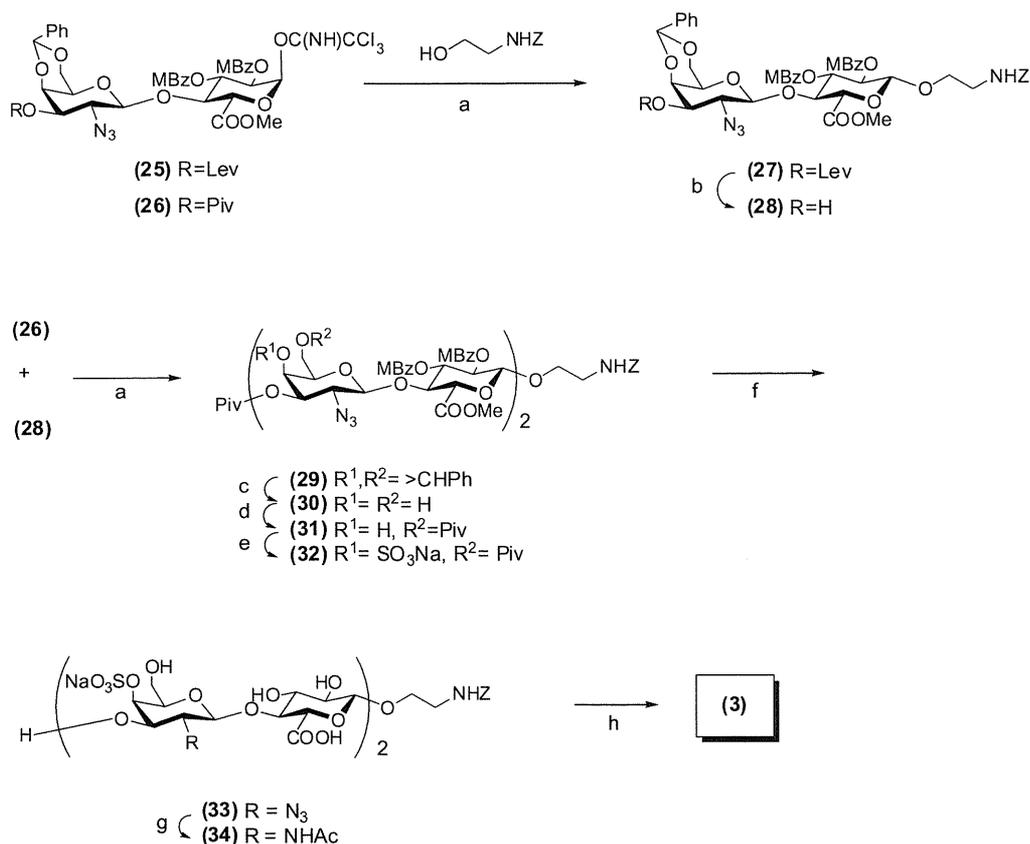
Scheme 3. Synthesis of **3**. Reagents and conditions: (a) TMSOTf, MSAW300, CH$_2$Cl$_2$, −20 °C to rt, 50% (for **27**), 43% (for **29**); (b)H$_2$NNH$_2$·AcOH, toluene–EtOH, 84%; (c) camphorsulfonic acid, CH$_2$Cl$_2$–MeOH, quant.; (d)PivCl, pyridine, quant.; (e)SO$_3$·NMe$_3$, DMF, 60 °C, 92%; (f) aq LiOH, THF, then aq NaOH, CH$_2$Cl$_2$–MeOH, quant.; (g)Zn, aq AcOH, 62%; (h) H$_2$, Pd–C, cat. AcOH, aq EtOH, then NHS–PEO$_4$–biotin, 0.1 M Na$_3$PO$_4$, 0.15 M NaCl, 58% (for 2 steps).

Table 1
K_D values for the interaction of the synthesized tetrasa-charides and midkine in the BIAcore system

CS-type	K_D (nM)
OO	2.03×10^3
AA	17.8
AE	11.6
EE	2.62

We prepared a tetrasaccharide (**8**) common to the three target compounds. The diaosyl trichloroacetimidate[8] was coupled with HO(CH$_2$)$_2$NHZ in the presence of TMSOTf to give **6** in 65% yield (Scheme 1). The levulinoyl group was chemoselectively removed with H$_2$NNH$_2$·AcOH to afford **7** in 77% yield. Another imidate having a pivaloyl ester at the non-reducing end (**5**)[9] was coupled with **7** in the same manner as for the synthesis of **6** to give the tetrasaccharide **8** in 58% yield. We removed both benzylidene acetals under acidic conditions to obtain **9** in a quantitative yield. Unprotected **12** was also quantitatively obtained by saponification of **9**. Subsequent hydrogenolysis afforded free amine (**14**) which was coupled with a biotin linker to obtain the target compound (**1**, 93%, 2 steps). Conversely, the tetraol (**9**) was sulfated with SO$_3$·NMe$_3$ in DMF at 60 °C to give **11** in 86% yield. The same saponification procedure afforded **13** in 97% yield. Subsequent hydrogenolysis and biotinylation gave the target compound (**2**, 69%, 2 steps).

We tried to obtain another target compound, CS-AA (**3**). The benzylidene acetal of **8** was reductively and regioselectively opened with selected amounts of BH$_3$·NMe$_3$, AlCl$_3$ and H$_2$O in

THF[12] to obtain **10** having di-O-benzyl ether at O-6 of both GalNAc residues in 13% yield. At the same time monobenzylated compounds having intact benzylidene acetals were obtained in 36% yield together with 30% of recovered **8**. However, subsequent sulfation at two 4-OHs of **10** was unsuccessful. Although TLC showed a complete change to a slower moving spot which suggested O-sulfation, ^{1}H NMR showed no downfielded signals for H-4[II] and 4[IV] (data not shown). The oxygen of the acetamide might be sulfated as we have already reported,[7] but no O-sulfation occurred even with a longer reaction time.

We re-examined the O-sulfation with a disaccharide having liberated 4-OH at the GalNAc residue (**20**) which was synthesized by regioselective pivaloylation at the primary position of **18**[7] with Piv-Cl in pyridine at −40 °C in 73% yield (Scheme 2). We observed a similar phenomenon on TLC during the sulfation of **20** and obtained a polar product in 92% yield (as a monosulfate) which was subjected to a saponification reaction. The final product proved to be non-sulfated **22**[7] (59% yield) as expected. This result indicates the polar product obtained by the sulfation to have an imine-like structure (**21**).

To avoid sulfation at the acetamide we changed the synthetic route as pictured in Scheme 2, employing azide instead of acetamide on the galactosamine residue. The benzylidene acetal of the known disaccharide (**16**)[7] was removed under acidic conditions to give **17** in 78% yield. We obtained **19** by the regioselective pivaloylation of **17** at 6-OH. The sulfation of **19** at 4-OH afforded sulfate (**23**) in 96% yield. The azide of **23** was successfully converted to acetamide with AcSH[13] to give **24** in 90% yield, thus proving that this strategy is reasonable for obtaining the 4-O-sulfated CS.

As shown in Scheme 3, the imidate (**25**)[8] having azide was stereoselectively coupled with HO(CH$_2$)$_2$NHZ in the same manner as for the synthesis of **6** to give **27** in 50% yield. The levulinoyl group of **27** was removed in 84% yield and the other imidate (**26**) was coupled in the same manner as above to afford the tetrasaccharide (**29**) in 43% yield. Two benzyliden acetals of **29** were removed to obtain **30** and the primary alcohols of which were pivaloylated to give **31** in a quantitative yield (2 steps). The two liberated hydroxyl groups were sulfated with SO$_3$·NMe$_3$ in DMF to give **32** in 92% yield. All the acyl groups were quantitatively removed by saponification to obtain **33**.

We then examined the chemoselective reduction of the azide of **33** in the presence of Z. Z is thought to usually resist hydrogenolysis in the presence of a Lindlar catalyst,[14] but was completely removed in our case. It seems that this reaction deeply depends on the lot of the reagent or degree of Pd by PbSO$_4$. An alternative Pd catalyst, Pd–C/Ph$_2$S,[15] afforded the same result. We also tried the reduction of azide with AcSH, but obtained a very low yield. Nakahara's group achieved the reduction of azide with Zn and AcOH in ethyl acetate.[16] We employed Zn in AcOH but this afforded a complicated reaction mixture. However, aq AcOH (AcOH: H$_2$O = 5:1) instead of glacial AcOH completely improved the reaction to give **34** in 62% yield after N-acetylation. The final removal of Z by hydrogenolysis and subsequent biotinylation at the non-reducing end as above afforded CS-AA (**3**) in 58% yield (2 steps). We confirmed the structures of **1–3** by ^{1}H NMR spectroscopy and TOF-MS.[17]

The tetrasaccharides having a biotin linker were immobilized on plates and their affinity for midkine was investigated.[18] We also prepared a CS-AE type substrate, GlcAβ-GalNAc(4S)β-GlcAβ-Gal-NAc(4S6S)β, by digestion with 6-O-sulfatase. Midkine exhibited interaction with these tetrasaccharides. The K_D values are summarized in Table 1. Midkine had the highest affinity for CS-EE among the tetraosyl biotins with other types of sulfation patterns. The K_D value of CS-AE is larger than that of CS-EE. It seems that the 6-O-sulfate at the non-reducing terminal is important for binding to midkine. The sulfate at the 4-position at the non-reducing end is also involved in the interaction with midkine.

In summary, we synthesized chondroitin sulfate tetrasaccharides having different sulfation patterns via the 2+2 coupling of disaccharide units. These oligosaccharides are linked to biotin via a hydrophilic linker. We clarified that midkine preferred the highly sulfated EE-type sequence to the AE, AA and OO-type chondroitin tetrasaccharides.

Acknowledgment

References and notes

1. Wang, H.; Katagiri, Y.; McCann, T. E.; Unsworth, E.; Goldsmith, P.; Yu, Z.-X.; Fei, T.; Santiago, L.; Mills, E. M.; Wang, Y.; Symes, A.; Geller, H. M. J. Cancer Sci. **2008**, 121, 3083.
2. Mikami, T.; Yasunaga, D.; Kitagawa, H. J. Biol. Chem. **2009**, 284, 4494.
3. Kawashima, H. Biol. Pharm. Bull. **2006**, 29, 2343.
4. Uyama, T.; Ishida, M.; Izumikawa, T.; Trybala, E.; Tufaro, F.; Bergström, T.; Sugahara, K.; Kitagawa, H. J. Biol. Chem. **2006**, 281, 38668.
5. Sugahara, K. N.; Hirata, T.; Tanaka, T.; Ogino, S.; Takeda, M.; Terasawa, H.; Shimada, I.; Tamura, J.; ten Dam, G. B.; van Kuppevelt, T. H.; Miyasaka, M. Cancer Res. **2008**, 68, 7191.
6. Yamamoto, H.; Muramatsu, H.; Nakanishi, T.; Natori, Y.; Sakuma, S.; Ishiguro, N.; Muramatsu, T. Biolchem. Biophys. Res. Commn. **2006**, 351, 915.
7. Tamura, J.; Neumann, K. W.; Kurono, S.; Ogawa, T. Carbohydr. Res. **1998**, 305, 43.
8. Tamura, J.; Tokuyoshi, M. Biosci. Biotech. Biochem. **2004**, 68, 2436.
9. Tamura, J.; Nakada, Y.; Taniguchi, K.; Yamane, M. Carbohydr. Res. **2008**, 343, 39.
10. Vibert, A.; Lopin-Bon, C.; Jacquinet, J.-C. Chem. Eur. J. **2009**, 15, 9561.
11. Vibert, A.; Lopin-Bon, C.; Jacquinet, J.-C. Eur. J. Org. Chem. **2011**, 4183.
12. Sherman, A. A.; Mironov, Y. V.; Yudina, O. N.; Nifantiev, N. E. Carbohydr. Res. **2003**, 338, 697.
13. Rosen, T.; Lico, I. M.; Chu, D. T. W. J. Org. Chem. **1988**, 53, 1580.
14. Wuts, P. G. M.; Green, T. W. Green's Protective Groups in Organic Synthesis; John Wiely & Sons: Weinheim, 2007.
15. Mori, A.; Mizusaki, T.; Kawase, M.; Maegawa, T.; Monguchi, Y.; Takao, S.; Takagi, Y.; Sajiki, H. Adv. Synth. Catal. **2008**, 350, 406.
16. Ueki, A.; Nakahara, Yu.; Hojo, H.; Nakahara, Yo. Tetrahedron **2007**, 63, 2170.
17. ^{1}H NMR assignments were confirmed by two-dimensional HH COSY experiments using BRUKER ADVANCE II 600 MHz spectrometers with tert-BuOH as an internal standard (1.23 ppm) in D$_2$O. As an example of signal assignments, 1^{III} stands for a proton at C-1 of sugar residue III. Positions of the protons in the aglycon are depicted in Scheme 1. Compound **1**: ^{1}H NMR: δ 4.60 (dd, 1H, $J_{b,c}$ = 7.86 Hz, $J_{c,d}$ = 5.04 Hz, H-c), 4.51 (br d, 2H, J = 7.98 Hz, H-1$^{I\ or\ III}$, 1^{IV}), 4.50 (br d, 1H, J = 6.67 Hz, H-1$^{III\ or\ I}$), 4.45 (d, 1H, $J_{1,2}$ = 8.40 Hz, H-1^{II}), 4.41 (dd, 1H, $J_{b,e}$ = 4.56 Hz, H-b), 4.09 (d, 1H, $J_{3,4}$ = 3.00 Hz, H-4^{IV}), 3.98 (dd, 1H, $J_{1,2}$ = 8.52 Hz, $J_{2,3}$ = 10.74 Hz, H-2^{IV}), 3.93 (m, 1H, H-r), 3.91 (d, 1H, $J_{3,4}$ = 3.12 Hz, H-4^{II}), 3.88 (d, 1H, $J_{4,5}$ = 9.79 Hz, H-5^{I}), 3.86 (dd, 1H, $J_{2,3}$ = 10.80 Hz, H-2^{II}), 3.83–3.65 (m, 7H, H-4$^{I,\ III}$, 5^{III}, 6$^{II,\ IV}$x4), 3.80 (m, 1H, H-3^{IV}), 3.76 (m, 5H, H-n, r), 3.68 (m, 2H, H-3^{I}, 5^{IV}), 3.68 (br s, 12H, H-m), 3.64–3.57 (m, 4H, H-3$^{I,\ III}$, I × 2), 3.43 (m, 4H, H-k, q), 3.36 (m, 2H, H-2$^{I,\ III}$), 3.32 (m, 1H, H-e), 2.98 (dd, 1H, J_{gem} = 13.02 Hz, H-d), 2.77 (d, 1H, H-d'), 2.52 (br t, 2H, J = 6.09 Hz, H-o), 2.26 (br t, 2H, J = 7.30 Hz, H-i), 2.02, 1.99 (2s, 3H × 2, 2NAc), 1.70 (m, 1H, H-f), 1.64 (m, 2H, H-h), 1.58 (m, 1H, H-f'), 1.40 (m, 2H, H-g).MALDI-TOFMS: m/z calcd for C$_{51}$H$_{84}$N$_6$O$_{30}$SNa, 1315.49; found, 1315.49 [M+Na$^+$].MALDI-TOFMS: m/z calcd for C$_{51}$H$_{84}$N$_6$O$_{30}$SNa, 1315.49; found, 1315.49 [M+Na$^+$].Compound **2**: ^{1}H NMR: δ 4.74 (s, 1H, H-4^{II}), 4.67 (d, 1H, $J_{3,4}$ = 2.28 Hz, H-4^{IV}), 4.59 (m, 2H, H-1^{II}, c), 4.54 (d, 1H, $J_{1,2}$ = 9.78 Hz, H-1^{IV}), 4.52 (d, 1H, $J_{1,2}$ = 9.72 Hz, H-1$^{I\ or\ III}$), 4.52 (d, 1H, $J_{1,2}$ = 7.74 Hz, H-1$^{III\ or\ I}$), 4.42 (dd, 1H, $J_{b,c}$ = 7.87 Hz, $J_{b,e}$ = 4.50 Hz, H-b), 4.02 (d, 1H, J = 9.78 Hz, H-5^{I}), 4.01 (brd, 1H, J = 3.90 Hz, H-2^{IV}), 3.95 (d, 1H, $J_{4,5}$ = 9.86 Hz, H-5^{III}), 3.92 (m, 1H, H-r), 3.88 (dd, 1H, $J_{2,3}$ = 12.43 Hz, H-2^{IV}), 3.86 (m, 1H, H-3^{IV}), 3.84–3.65 (m, 6H, H-5$^{II,\ IV}$, 6$^{II,\ IV}$ × 2), 3.82 (m, 2H, H-4$^{I,\ III}$), 3.81 (m, 1H, H-3^{II}), 3.77 (m, 3H, H-n, r), 3.67 (m, 14H, H-3$^{I,\ III}$, m), 3.62 (m, 2H, H-I), 3.42 (m, 4H, H-k, q), 3.38 (m, 2H, H-2$^{I,\ III}$), 3.33 (m, 1H, H-e), 2.99 (dd, 1H, J_{gem} = 13.08 Hz, $J_{c,d}$ = 4.98 Hz, H-d), 2.77 (d, 1H, H-d'), 2.52 (t, 2H, J = 6.15 Hz, H-o), 2.27 (t, 2H, J = 7.32 Hz, H-i), 2.02, 2.00 (2s, 3H × 2, 2NAc), 1.72 (m, 1H, H-f), 1.62 (m, 2H, H-h), 1.59 (m, 1H, H-f'), 1.41 (m, 2H, H-g). MALDI-TOFMS: m/z calcd for C$_{51}$H$_{80}$N$_6$O$_{42}$S$_5$Na$_5$, 1723.19; found, 1723.24 [M+Na$^+$]. Compound **3**: ^{1}H NMR: δ 4.76 (m, 1H, H-4^{II}), 4.71 (d, 1H, $J_{3,4}$ = 2.10 Hz, H-4^{IV}), 4.62 (m, 1H, H-1^{II}), 4.60 (m, 1H, H-c), 4.60 (m, 1H, $J_{1,2}$ = 7.80 Hz, H-1^{IV}), 4.55 (d, 1H, $J_{1,2}$ = 7.98 Hz, H-1$^{I\ or\ III}$), 4.54 (d, 1H, $J_{1,2}$ = 7.92 Hz, H-1$^{III\ or\ I}$), 4.42 (dd, 1H, $J_{b,c}$ = 7.92 Hz, $J_{b,e}$ = 4.50 Hz, H-b), 4.29–4.20 (m, 4H, H-6$^{II,\ IV}$ × 2), 4.11 (m, 2H, H-5$^{II,\ IV}$), 4.03 (m, 2H, H-2^{II},3^{II}), 4.02 (d, 1H, J = 9.66 Hz, H-5^{I}), 3.97 (d, 1H, $J_{4,5}$ = 9.78 Hz, H-5^{III}), 3.92 (m, 1H, H-r), 3.88 (m, 2H, H-2^{IV}, 3^{IV}), 3.83 (m, 2H, H-4$^{I,\ III}$), 3.77 (m, 3H, H-n, r), 3.71–3.64 (m, 14H, H-3$^{I,\ III}$, m), 3.62 (t, 2H, J = 5.34 Hz, H-I), 3.42 (m, 4H, H-k, q), 3.39 (m, 2H, H-2$^{I,\ III}$), 3.33 (m, 1H, H-e), 2.99 (dd, 1H, J_{gem} = 13.08 Hz, $J_{c,d}$ = 4.98 Hz, H-d), 2.77 (d, 1H, H-d'), 2.52 (t, 2H, J = 6.09 Hz, H-o), 2.27 (t, 2H, J = 7.30 Hz, H-i), 2.02, 2.00 (2s, 3H × 2, 2NAc), 1.72 (m, 1H, H-f), 1.64 (m, 2H, H-h), 1.57 (m, 1H, H-f'), 1.41 (m, 2H, H-g).
18. Streptavidin-coated sensor chip (Sensor Chip SA)(GE Healthcare) was washed with 1 M NaCl at a flow rate of 30 μl/min according to the manufacture's instructions. Biotinylated tetrasaccharides diluted in HBS-EP buffer (10 mMHEPES, 0.15 M NaCl, 3.4 mM EDTA, 0.005% surfactant P20, pH 7.4) were perfused and allowed to interact with the surface of the sensor at a flow rate of 30 μl/min. Kinetic analyses were performed using a range of recombinant midkine concentrations (90, 180, and 360 nM)at 30 μl/min. Midkine was applied to the sensor chip (30 μl/min) for 2 min and left to dissociate for 3 min. Surfaces were regenerated using 1 M NaCl. Data were analyzed by BIA evaluation 3.0 software using a 1:1 Langmuir binding model.

nature
neuroscience

Persistent cortical plasticity by upregulation of chondroitin 6-sulfation

Shinji Miyata[1,2], Yukio Komatsu[3], Yumiko Yoshimura[4], Choji Taya[5] & Hiroshi Kitagawa[1,2]

Cortical plasticity is most evident during a critical period in early life, but the mechanisms that restrict plasticity after the critical period are poorly understood. We found that a developmental increase in the 4-sulfation/6-sulfation (4S/6S) ratio of chondroitin sulfate proteoglycans (CSPGs), which are components of the brain extracellular matrix, leads to the termination of the critical period for ocular dominance plasticity in the mouse visual cortex. Condensation of CSPGs into perineuronal nets that enwrapped synaptic contacts on parvalbumin-expressing interneurons was prevented by cell-autonomous overexpression of chondroitin 6-sulfation, which maintains a low 4S/6S ratio. Furthermore, the increase in the 4S/6S ratio was required for the accumulation of Otx2, a homeoprotein that activates the development of parvalbumin-expressing interneurons, and for functional maturation of the electrophysiological properties of these cells. Our results indicate that the critical period for cortical plasticity is regulated by the 4S/6S ratio of CSPGs, which determines the maturation of parvalbumin-expressing interneurons.

Ocular dominance plasticity is a classic example that has been used to study the effects of experience on cortical circuits[1,2]. Brief monocular deprivation leads to a reduction in the responses of visual cortical neurons to the deprived eye and an increase in the responses to the nondeprived eye. Sensitivity to monocular deprivation is high in juvenile animals during a critical period in early life (postnatal days 19–32 (P19–32) in the mouse visual cortex), after which cortical neurons become less plastic[3]. Considerable evidence indicates that functional changes in the balance between excitation and inhibition control ocular dominance plasticity[2]. In particular, maturation of a subset of inhibitory interneurons expressing the calcium-binding protein parvalbumin has been proposed to be crucial for defining the timing of the critical period[2,4,5].

CSPGs consist of a core protein with covalently attached chondroitin sulfate glycosaminoglycan chains (**Fig. 1a**) and are major components of the brain extracellular matrix[6]. During postnatal development, CSPGs condense around the soma and proximal dendrites of parvalbumin-expressing interneurons, forming perineuronal nets (PNNs), a specialized extracellular matrix structure that interdigitates with synaptic contacts[7]. PNNs are composed of several CSPGs and hyaluronan, and the interaction between CSPGs and hyaluronan is stabilized by tenascin-R and cartilage link proteins[8]. Although the cellular origins of their components are not fully understood, both neurons and glial cells may contribute to the formation of PNNs[9]. Digestion of chondroitin sulfate chains with chondroitinase ABC disrupts PNNs and reactivates ocular dominance plasticity in adult animals after the closure of the critical period, indicating that the chondroitin sulfate moieties of CSPGs are responsible for PNN formation and control of the critical period plasticity[10]. It has been

suggested that chondroitin sulfate chains present a physical barrier that limits the critical period plasticity by preventing rearrangements of synaptic connections because they inhibit axonal sprouting and regeneration after nerve injury[11]. However, it is unlikely that all chondroitin sulfate chains inherently inhibit plasticity, as chondroitin sulfate chains are very abundant, even in the juvenile brain during the critical period.

Recent studies have proposed that the functional information of CSPGs is encoded by the specific sulfation sequence of chondroitin sulfate chains[6,12–14]. Chondroitin sulfate chains are long linear polysaccharides that are composed of a repeating disaccharide unit that consists of glucuronic acid and N-acetylgalactosamine (GalNAc)[6]. During biosynthesis, GalNAc residues of the repeating disaccharide units are sulfated at C6 and C4 by chondroitin 6-sulfotransferase-1 (C6ST-1) and chondroitin 4-sulfotransferase-1 (C4ST-1), respectively (**Fig. 1a**). Chondroitin sulfate chains can act as both inhibitory molecules for axonal growth and neuritogenic molecules depending on their sulfation status[6,13]. Previously, we found that the neuritogenic effect of particular chondroitin sulfate chains was mediated by specific interaction with a cell adhesion molecule, contactin-1 (ref. 13). Despite increasing *in vitro* evidence that chondroitin sulfate chains act in a sulfation pattern–dependent manner, the role of CSPG sulfation patterns in cortical plasticity has garnered little attention. Specifically, the relationship between sulfation patterns of chondroitin sulfate and functional maturation of inhibitory interneurons has not been addressed. Moreover, the importance of specific sulfation patterns of chondroitin sulfate to cortical plasticity may have been overlooked in previous studies of chondroitin sulfate and plasticity because chondroitinase ABC treatment destroys all chondroitin

−156−

ARTICLES

sulfate chains, irrespective of sulfation status. The 4S/6S ratio changes during several biological processes[15,16]; thus, we hypothesized that sulfation patterns of chondroitin sulfate regulate the critical period plasticity. To test this hypothesis, we generated transgenic mice that overexpress human C6ST-1, a sulfotransferase catalyzing the 6-sulfation of chondroitin sulfate chains, under the control of a chicken β-actin promoter.

RESULTS

Sulfation patterns of chondroitin sulfate in mouse brain

We initially examined sulfation patterns of chondroitin sulfate in the developing mouse brain. Chondroitin sulfate chains isolated from mouse brain at different ages were digested with chondroitinase ABC and the resultant disaccharides were analyzed by high-performance liquid chromatography (**Supplementary Table 1**). In wild-type mice, the proportion of chondroitin 6-sulfation gradually decreased, whereas that of chondroitin 4-sulfation progressively increased (**Fig. 1b,c**), which resulted in a sharp increase in the 4S/6S ratio during development (**Fig. 1d**). In adult wild-type brain, chondroitin sulfate chains were mostly composed of chondroitin 4-sulfation, with chondroitin 6-sulfation only accounting for 2% of the total chondroitin sulfate. C6ST-1 (also known as CHST3) transgenic mice showed an increased proportion of chondroitin 6-sulfation and a decreased proportion of chondroitin 4-sulfation throughout development relative to control mice. The 4S/6S ratio in C6ST-1 transgenic mice was substantially lower than the ratio in control mice from P14 onward. Although the sulfation patterns of chondroitin sulfate changed markedly, the total

amount of chondroitin sulfate remained constant during development and did not differ between C6ST-1 transgenic and wild-type mice (**Fig. 1e**).

We also found that the developmental shift of the 4S/6S ratio correlated with the maturation timing of cortical regions. The 4S/6S ratio shift in the visual cortex occurred after that in the somatosensory cortex (**Fig. 1f**), which is consistent with the later maturation of the visual cortex[17]. Raising animals in complete darkness (dark rearing) delays the onset and termination of the critical period for ocular dominance plasticity in the visual cortex[2]. However, the 4S/6S ratio in the visual cortex was not affected by dark rearing (control, $n = 4$, 4S/6S ratio = 16.8 ± 0.39; dark rearing, $n = 4$, 4S/6S ratio = 15.9 ± 0.30; $P > 0.1$), suggesting that the temporal shift of the 4S/6S ratio is developmentally programmed, but is not dependent on visual experience. On the basis of immunohistochemical analysis using CS56 antibody that recognizes chondroitin 6-sulfation–related structures[18], we found that the shift in the sulfation patterns of chondroitin sulfate in C6ST-1 transgenic mice was delayed relative to that in wild-type mice (**Fig. 1g**), which is consistent with the results of our chemical disaccharide composition analysis. These results indicate that the sulfation patterns, but not the amount of chondroitin sulfate chains, changed during the critical period and that C6ST-1 transgenic mice retain immature sulfation patterns of chondroitin sulfate throughout life.

C6ST-1 transgenic adults retain ocular dominance plasticity

To investigate whether the sulfation patterns of chondroitin sulfate influence the onset of the critical period, we assessed ocular dominance
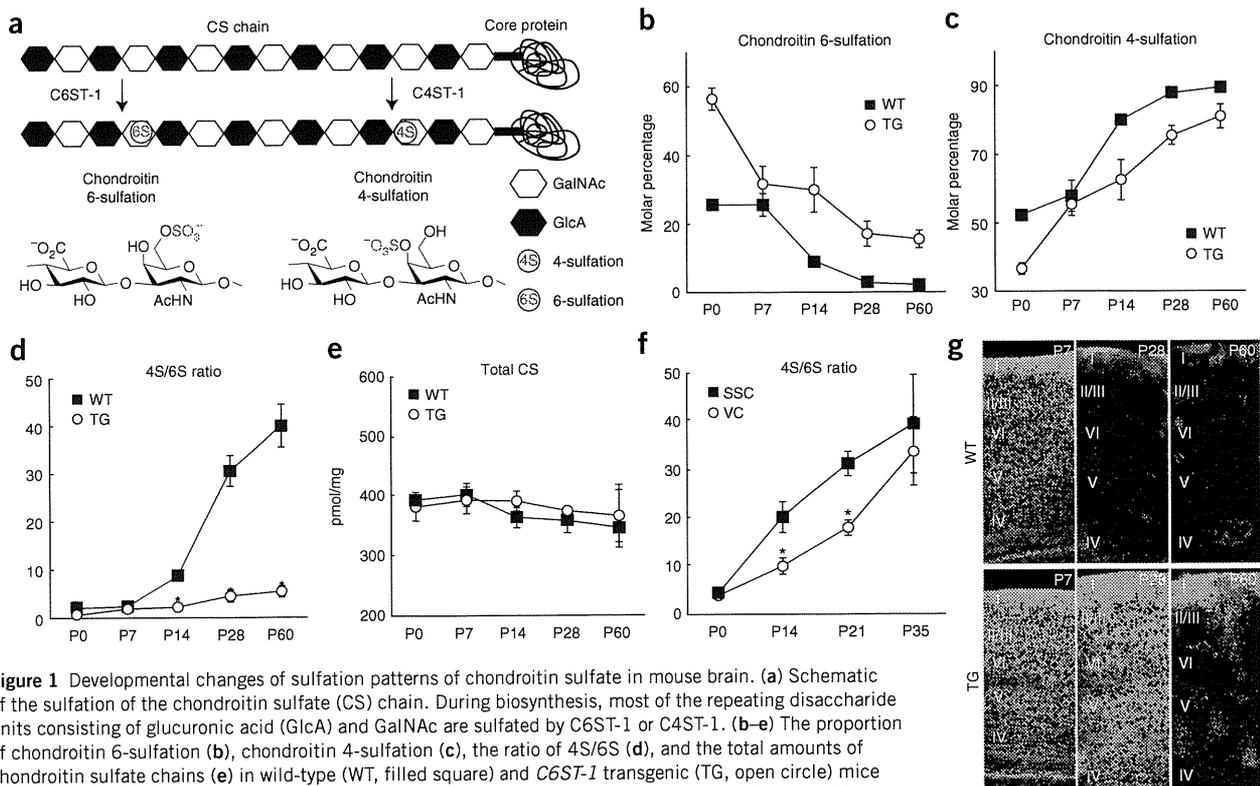
Figure 1 Developmental changes of sulfation patterns of chondroitin sulfate in mouse brain. (**a**) Schematic of the sulfation of the chondroitin sulfate (CS) chain. During biosynthesis, most of the repeating disaccharide units consisting of glucuronic acid (GlcA) and GalNAc are sulfated by C6ST-1 or C4ST-1. (**b–e**) The proportion of chondroitin 6-sulfation (**b**), chondroitin 4-sulfation (**c**), the ratio of 4S/6S (**d**), and the total amounts of chondroitin sulfate chains (**e**) in wild-type (WT, filled square) and C6ST-1 transgenic (TG, open circle) mice during development. Molar percentages in **b** and **c** were calculated by dividing the amount of chondroitin 6- and 4-sulfation, respectively, by the total amount of disaccharides. The 4S/6S ratio was calculated by dividing the molar percentage of chondroitin 4-sulfation by that of chondroitin 6-sulfation. (**f**) The ratio of 4S/6S in the somatosensory cortex (SSC, filled square) and visual cortex (VC, open circle) in wild-type mice. Error bars represent s.d. ($n = 3$ for each point). *$P < 0.05$ (Student's t test) between the two groups at the same time point. (**g**) C6ST-1 transgenic mice showed a delayed decrease in CS56 staining in the developing visual cortex. Cortical layers are indicated with Roman numerals on the left. Scale bar represents 100 μm.

Figure 2 Sulfation patterns of chondroitin sulfate participate in the termination of the critical period. (**a**) Monocular deprivation periods of 3 or 6 d beginning at P24–26 resulted in a significant decrease in the contralateral/ipsilateral (C/I) ratio in both wild-type and C6ST-1 mice as compared with nondeprived (No MD) mice. (**b**) In both groups, 3-d monocular deprivation depressed responses to the deprived eye (open bars) and 6-d monocular deprivation potentiated responses to the nondeprived eye (filled bars) (No MD: wild type $n = 12$, C6ST-1, $n = 10$; 3-d monocular deprivation: wild type $n = 18$, C6ST-1, $n = 14$; 6-d monocular deprivation: wild type $n = 12$, C6ST-1, $n = 11$). (**c**) In adulthood (P60–90), 3-d monocular deprivation did not affect the contralateral/ipsilateral ratio in wild-type mice, but did induce a significant contralateral/

ipsilateral shift in C6ST-1 mice. 6 d of monocular deprivation caused a significant contralateral/ipsilateral shift in both groups. (**d**) In wild-type mice, 6-d monocular deprivation induced potentiation of the responses to the nondeprived eye (filled bars), but no change in the responses to the deprived eye (open bars). C6ST-1 mice showed depression in the responses to the deprived eye and potentiation of the responses to nondeprived eye (No MD: wild type $n = 11$, C6ST-1, $n = 12$; 3-d monocular deprivation: wild type $n = 10$, C6ST-1, $n = 11$; 6-d monocular deprivation: wild type $n = 8$, C6ST-1, $n = 14$). $*P < 0.05$ (Student's t test) from No MD groups. Error bars represent s.e.m. Representative waveforms of VEPs are shown at the top of **b** and **d**. Scale bars represent 100 ms and 100 µV.
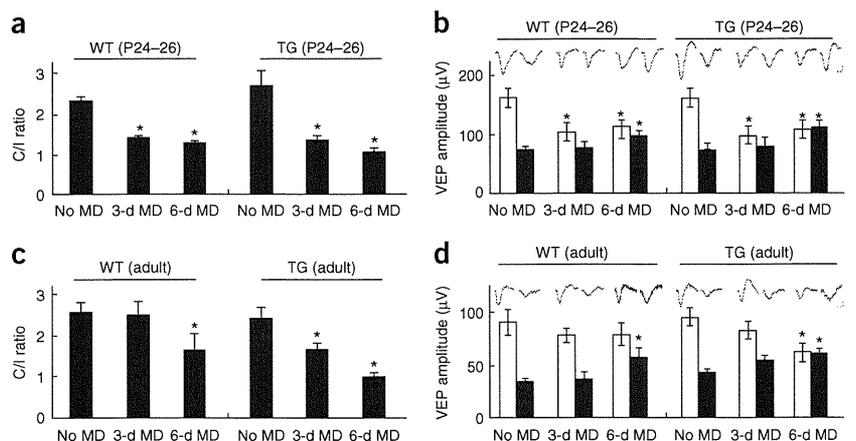
plasticity by recording visual evoked potentials (VEPs) from the binocular zone of the primary visual cortex. In both groups, the baseline ratio of contralateral eye VEP amplitude to ipsilateral eye VEP amplitude (the contralateral/ipsilateral ratio) was approximately 2, reflecting the contralateral eye dominance (**Fig. 2a**). We found that a 3- or 6-d monocular deprivation from P24–26 (the peak of the critical period) resulted in a significantly decreased contralateral/ipsilateral ratio in both groups ($P < 0.05$; **Fig. 2a**). Comparison of VEP amplitudes before and after monocular deprivation revealed two temporally distinct mechanisms for ocular dominance shift, as have been reported previously[19]. In both groups, the decrease in the contralateral/ipsilateral ratio was mediated by rapid depression of the responses to the deprived eye and by delayed potentiation of the responses to the nondeprived eye (**Fig. 2b**). Eye-specific projections from the retina to the dorsal lateral geniculate nucleus (dLGN) are known to be established in the first postnatal week[20]. C6ST-1 transgenic mice had normal eye-specific segregation of retinogeniculate axon terminals in the dLGN (**Supplementary Fig. 1**). Together, these results suggest that the initial construction of visual pathway and the onset of the critical period occur normally in C6ST-1 transgenic mice.

We next explored the effect of an altered sulfation pattern of chondroitin sulfate on the termination of the critical period. A 3-d monocular deprivation period did not alter the contralateral/ipsilateral ratio in wild-type adults as it had in juvenile mice (**Fig. 2c**). However, C6ST-1 transgenic adults did experience a significant contralateral/ipsilateral shift ($P = 0.02$) following 3 d of monocular deprivation imposed after the critical period. Although recent studies have suggested that a longer period of monocular deprivation can induce a weak shift in the contralateral/ipsilateral ratio in adult animals, the nature of juvenile and adult ocular dominance plasticity is markedly different[21]. In wild-type adults, 6 d of monocular deprivation caused a mild, but statistically significant ($P < 0.05$), contralateral/ipsilateral shift that was mainly mediated by increased responses to the nondeprived eye, rather than by decreased responses to the deprived eye (**Fig. 2d**). This indicates that depression in responses to the deprived eye in wild-type mice is restricted to the critical period. In contrast, the contralateral/ipsilateral shift in C6ST-1 transgenic adults caused by 6 d of monocular deprivation resulted from both depression in

responses to the deprived eye and potentiation of responses to the nondeprived eye, which is similar to that observed in juvenile mice. These results suggest that C6ST-1 transgenic adults retain juvenile-like ocular dominance plasticity.

C6ST-1 transgenic mice have reduced PNNs formation

We next examined whether the sulfation patterns of chondroitin sulfate affected formation of PNNs using a well-established marker, *Wisteria floribunda* agglutinin (WFA)[22]. During the first postnatal week, CSPGs were diffusely distributed and no PNN was observed in the visual cortex (**Fig. 3**). Formation of WFA$^+$ PNNs began around P14, gradually increased after the critical period and displayed a time course similar to the shift in the 4S/6S ratio (**Fig. 3a,b**). In the visual cortex of wild-type adults, most parvalbumin-expressing interneurons (90%) were surrounded by WFA$^+$ PNNs. Notably, C6ST-1 transgenic mice showed a significantly reduced ($P = 0.002$ for P28, $P = 0.0005$ for adults) number of WFA$^+$ PNNs during and after the critical period (**Fig. 3a,c**); however, the number of parvalbumin-expressing interneurons was similar in wild-type and C6ST-1 transgenic mice (**Fig. 3a,d**). This indicates that developmental changes in sulfation patterns of chondroitin sulfate are required for normal formation of PNNs.

Notably, some parvalbumin-expressing interneurons (10%) in C6ST-1 transgenic mice were enwrapped by a distinct PNN-like structure that was recognized by CS56 antibody (**Fig. 3e**). These CS56$^+$ PNNs rarely colocalized with conventional WFA$^+$ PNNs in C6ST-1 transgenic mice and were not observed in wild-type controls (**Fig. 3f**). Thus, the lack of WFA staining does not necessarily mean the absence of PNNs in C6ST-1 transgenic mice. Instead, subpopulation of parvalbumin-expressing interneurons was surrounded by chondroitin 6-sulfation–enriched PNNs. Western blot analysis showed that the overall quantity of various core proteins, including aggrecan, a major CSPG in PNNs[23], were not altered in C6ST-1 transgenic mice (**Supplementary Fig. 2**), indicating that abnormal formation of PNNs in C6ST-1 transgenic mice is not a result of the reduced expression of PNN components. These results indicate that overexpression of C6ST-1 reduces the formation of conventional WFA$^+$ PNNs and increases the number of CS56$^+$ PNNs rich in chondroitin 6-sulfation around parvalbumin-expressing interneurons.

−158−

Figure 3 Impaired PNNs formation in *C6ST-1* mice. (a) Adult *C6ST-1* mice showed decreased formation of WFA[+] PNNs relative to controls. Right, high-magnification images of parvalbumin (PV)-expressing interneurons with or without (arrowhead) WFA[+] PNNs. (b) WFA[+] PNNs (red) first appeared at P14 in the visual cortex of wild-type mice. Nuclei were counterstained with Hoechst (blue). Cortical layers are indicated with Roman numerals on the left. (c,d) The number of WFA[+] PNNs (c), but not parvalbumin-expressing interneurons (d) in *C6ST-1* mice (closed bars) was significantly less than controls (open bars) throughout life. *P < 0.005 (Student's *t* test) between control versus *C6ST-1* transgenic for P28 and adult (P60–90), and P28 versus adult for control and *C6ST-1* transgenic. Error bars represent s.e.m.; n = 4–9. (e) Subpopulation of parvalbumin-expressing interneurons were surrounded by chondroitin 6-sulfation–enriched CS56^{+} PNNs (arrowheads) in *C6ST-1* mice. (f) CS56^{+} PNNs (arrowheads) were not colocalized with conventional WFA[+] PNNs in *C6ST-1* mice and were not observed in wild-type mice. Scale bars represent 100 μm (left panels in **a,b**), 10 μm (right panels in **a**) and 50 μm (**e,f**).
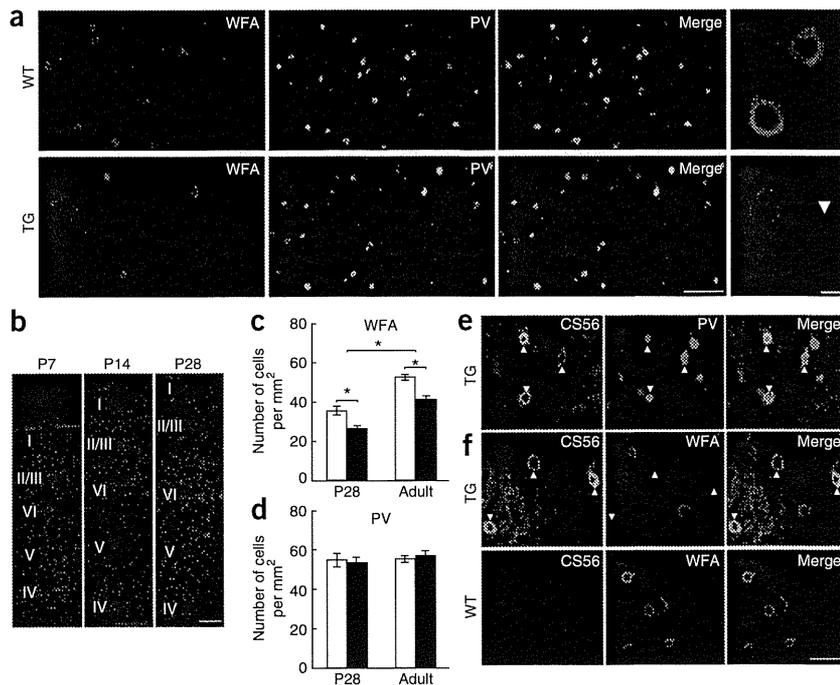
Sulfation patterns of PNNs regulate accumulation of Otx2

How could the sulfation patterns of chondroitin sulfate in PNNs influence critical period plasticity? The Otx2 homeoprotein was recently shown to regulate ocular dominance plasticity via its effects on maturation of parvalbumin-expressing interneurons[5]. Previous data suggest that Otx2 protein produced in the retina and dLGN is transported to the visual cortex via thalamocortical axons, secreted from thalamocortical terminals and internalized by postsynaptic parvalbumin-expressing interneurons[5]. However, because less than 20% of all thalamocortical synapses contact inhibitory interneurons, including parvalbumin-expressing interneurons[24], it is unclear how Otx2 selectively accumulates in parvalbumin-expressing interneurons. Thus, we tested whether the sulfation patterns of PNNs around parvalbumin-expressing interneurons affect the incorporation of Otx2. In the visual cortex of wild-type mice, Otx2 protein first became evident in parvalbumin-expressing interneurons during the critical period, and the number of Otx2^{+} cell was substantially increased by adulthood (**Fig. 4a,b**). Notably, there were significantly fewer (*P* = 0.001 for P28, *P* = 0.0002 for adults) Otx2^{+} cells in *C6ST-1* transgenic mice than in wild-type mice (**Fig. 4a,b**). Otx2 was mostly detected in parvalbumin-expressing interneurons surrounded by WFA[+] PNNs, but was not observed in parvalbumin-expressing interneurons surrounded by CS56^{+} PNNs (**Fig. 4c**), suggesting that the accumulation of Otx2 was dependent on the sulfation patterns of chondroitin sulfate in PNNs. Closer observation revealed that Otx2 was distributed in a punctate pattern in the soma and proximal dendrites of parvalbumin-expressing interneuron (**Fig. 4d**). Otx2-immnopositive puncta did not overlap with, but were closely apposed to, WFA[+] PNNs. The expression of *Otx2* mRNA in the retina and dLGN was indistinguishable between the two groups, excluding the possibility that overexpression of C6ST-1 affects expression of *Otx2* transcripts (**Supplementary Fig. 3**). Neither wild-type nor *C6ST-1* transgenic mice expressed detectable levels of *Otx2* mRNA in the visual cortex.

We further analyzed the spatial relationship between PNNs and thalamocortical synaptic contact sites in layer 4, which receives most of

the thalamocortical input. Three-dimensional reconstruction of WFA[+] PNNs revealed a distinct meshwork surrounding soma and proximal dendrites of parvalbumin-expressing interneurons in wild-type mice (**Fig. 5a**). We selectively labeled thalamocortical boutons using antibody against vesicular glutamate transporter 2 (VGluT2)[24]. The holes in the meshwork of WFA[+] PNNs were evidently the areas occupied by thalamocortical boutons. In contrast, CS56^{+} PNNs showed sparse dot-like particles rather than a meshwork structure, and thalamocortical boutons projecting onto parvalbumin-expressing interneurons in *C6ST-1* transgenic mice were not surrounded by PNNs (**Fig. 5a**). Because both WFA lectin and CS56 antibody recognize the chondroitin sulfate moiety of CSPGs, we stained WFA[+] and CS56^{+} PNNs with an antibody recognizing the core protein portion of aggrecan. This confirmed the meshwork structure of WFA[+] PNNs in controls and the diffusely spread and less condensed morphology of CS56^{+} PNNs in *C6ST-1* transgenic mice (**Fig. 5b**). These results indicate that diffuse PNNs that are rich in chondroitin 6-sulfation may be unable to tightly surround thalamocortical synaptic contacts, leading to diffusion and reduced accumulation of Otx2 at these contacts.

Overexpression of C6ST-1 in inhibitory interneurons

To address the cellular origin of the abnormal PNNs formation in *C6ST-1* transgenic mice, we carried out two series of experiments. First, we assessed the possible contribution of astrocytes to the formation of CS56^{+} PNNs using a heterologous neuron and astrocyte co-culture system. We found that parvalbumin-expressing interneurons were surrounded by CS56^{+} PNNs when cortical neurons from *C6ST-1* transgenic, but not wild type, mice were grown on an astrocyte monolayer, regardless of the origin of the astrocytes (**Supplementary Fig. 4**). This suggests that overexpression of C6ST-1 in neurons, but not in astrocytes, is required for the formation of CS56^{+} PNNs.

Second, we sought to directly determine whether cell-autonomous upregulation of chondroitin 6-sulfation in parvalbumin-expressing interneurons induces the formation of CS56^{+} PNNs *in vivo*. In contrast with excitatory pyramidal neurons that are born in the

Figure 4 Sulfation patterns of chondroitin sulfate–dependent accumulation of Otx2 homeoprotein in parvalbumin-expressing interneurons. (a) In adult visual cortex, C6ST-1 mice had reduced accumulation of Otx2 in parvalbumin-expressing interneurons as relative to controls. (b) Quantitative analysis of the number of Otx2^{+} cells in wild-type (open bars) and C6ST-1 (closed bars) mice. *P < 0.05 (Student's t test) between P28 versus adult for control and control versus C6ST-1 transgenic for P28 and adult. Error bars represent s.e.m. (n = 3–6). (c) Otx2 (arrowheads) accumulated in parvalbumin-expressing interneurons surrounded by WFA[+] PNNs in controls, but not in parvalbumin-expressing interneurons surrounded by CS56^{+} PNNs (arrows) in C6ST-1 mice. (d) Otx2-immnopositive puncta in parvalbumin-expressing interneurons closely apposed to WFA[+] PNNs. Scale bars represent 100 μm (a,c) and 2 μm (d).
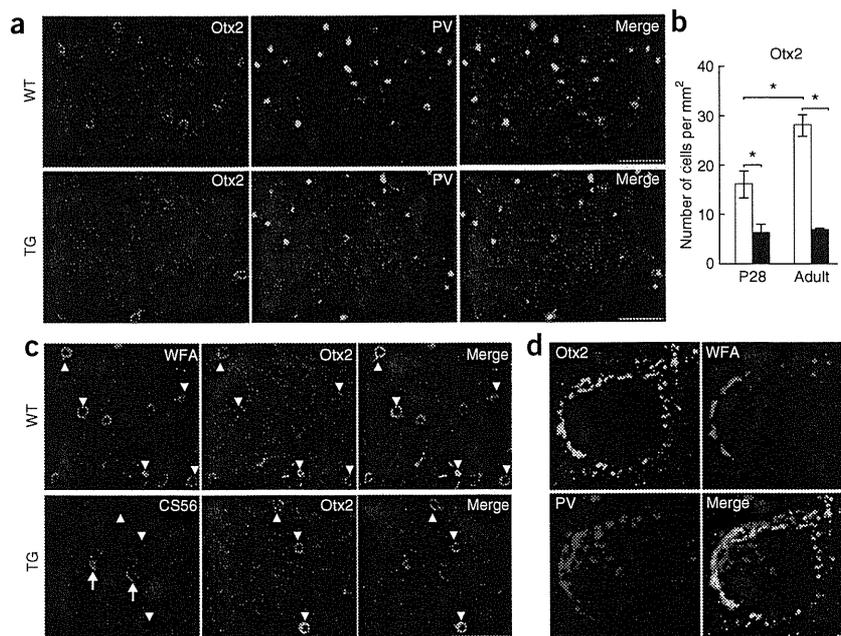
cortical proliferative zones, inhibitory interneurons, including parvalbumin-expressing interneurons, originate from the ganglionic eminences and migrate tangentially into the cortex[25]. Thus, to achieve interneuron-specific gene expression, we performed ganglionic eminence–directed in utero electroporation[26,27] with C6ST-1–expressing and yellow fluorescence protein (YFP)-expressing plasmids at embryonic day 12.5 (E12.5; **Fig. 6a**). Immunohistochemical analysis of the postnatal cortex at P30 showed that 26% of transfected neurons (n = 24 of 91 YFP-positive neurons) were immunoreactive for parvalbumin (**Fig. 6b**). Notably, in contrast with untransfected control parvalbumin-expressing interneurons, most C6ST-1–transfected parvalbumin-expressing interneurons were surrounded by CS56^{+} PNNs (88%, n = 21 of 24 YFP and parvalbumin double-positive neurons; **Fig. 6b**). As observed in C6ST-1 transgenic mice, Otx2 was not accumulated in parvalbumin-expressing interneurons surrounded by CS56^{+} PNNs (0%, n = 0 of 20 YFP and CS-56 double-positive neurons; **Fig. 6c**). No CS56^{+} PNNs were formed when C6ST-1 was overexpressed in excitatory pyramidal neurons (**Fig. 6d**). These results indicate that PNNs formation and Otx2 accumulation were locally affected by parvalbumin-expressing interneuron autonomous production of

chondroitin 6-sulfation. In addition, these results suggest that sulfation patterns of chondroitin sulfate are involved in the uptake of Otx2 at the postsynaptic level, but not at the presynaptic level (for example, transport from subcortical to cortical areas and secretion from presynaptic terminals).

Electrophysiological properties of visual cortical neurons

We then asked what kinds of changes are produced in the electrophysiological properties of parvalbumin-expressing interneurons by overexpression of C6ST-1 using slice preparations of visual cortex at P30–34, after the peak of ocular dominance plasticity. Whole-cell recordings were conducted from nonpyramidal neurons located in or near layer 4 with patch pipettes containing biocytin in the current-clamp mode. We analyzed fast-spiking cells, as parvalbumin-expressing interneurons are practically equivalent to fast-spiking cells[28]. We encountered cells showing spike discharges that were characteristic of fast-spiking cells in C6ST-1 transgenic, as well as in wild-type, mice.

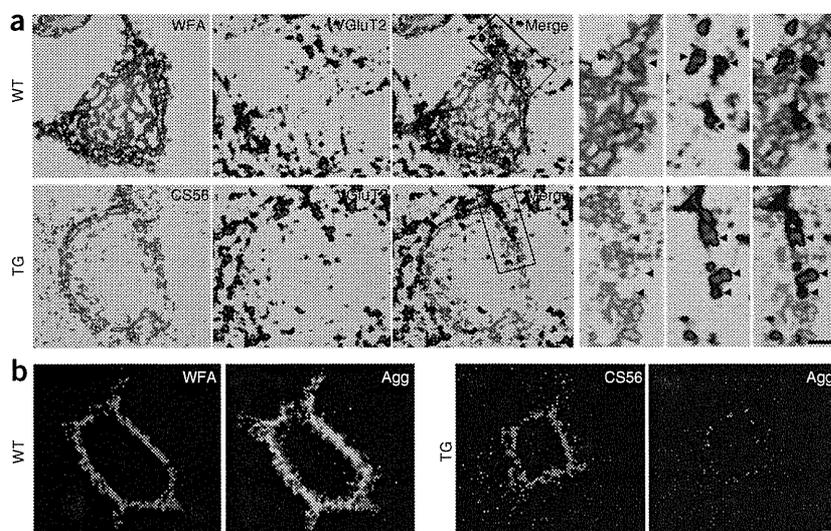A relative lack of spike-frequency adaptation during repetitive firing, a characteristic

Figure 5 Chondroitin 6-sulfation–enriched PNNs show a diffuse structure and are unable to tightly surround thalamocortical synaptic contacts. (a) Three-dimensional reconstruction revealed a distinct meshwork of WFA[+] PNNs in controls. In contrast, CS56^{+} PNNs in C6ST-1 mice were sparse dot-like structures. Right, magnification of boxed regions in the left panels. VGluT2-labeled thalamocortical boutons (arrowheads) were embedded in the meshwork of WFA[+] PNNs in controls, whereas these boutons were not surrounded by CS56^{+} PNNs in C6ST-1 mice. (b) Staining with antibody to aggrecan (Agg) revealed a well-formed meshwork and almost the same pattern as that with WFA lectin in controls. In contrast, aggrecan staining of CS56^{+} PNNs in C6ST-1 mice appeared diffuse and less condensed over the soma. Scale bars represent 2 μm.

–160–